Communications Research Centre

A TRANSPORTABLE LOW FREQUENCY COMMUNICATIONS SYSTEM

by

W.M. Evans

DEPARTMENT OF COMMUNICATIONS
MINISTÈRE DES COMMUNICATIONS

CRC REPORT NO. 1213

CANADA

OTTAWA, AUGUST 1971

COMMUNICATIONS RESEARCH CENTRE

DEPARTMENT OF COMMUNICATIONS
CANADA

A TRANSPORTABLE LOW FREQUENCY COMMUNICATIONS SYSTEM

by

W.M. Evans

(National Communications Laboratory)

Published August 1971
OTTAWA

CRC REPORT NO. 1213
DRB PROJECT NO. 7603
DRB TELS REPORT NO. 6

71-292

TABLE OF CONTENTS

1. INTRODUCTION 1
   1.1 Requirements 1
   1.2 Possible Solutions 2
   1.3 Portable LF Arctic Communications System 3

2. LOW FREQUENCY SYSTEM DESIGN 3
   2.1 Introduction 3
   2.2 Required RMS Carrier/RMS Noise 3
   2.3 Atmospheric Noise 4
   2.4 Man-Made Noise 4
   2.5 Required Signal Levels at Receiver Terminal 5
   2.6 Ground Wave Propagation Attenuation 5
   2.7 Required Radiated Power 7
   2.8 Summary of System Design 8

3. TRANSMITTING ANTENNA 9
   3.1 Introduction 9
   3.2 Transmitting Antenna Characteristics 9

4. COMMUNICATIONS TERMINAL DESCRIPTION 11
   4.1 Introduction 11
   4.2 Low Frequency Solid-State Transmitter 11
   4.3 LF Solid-State Receiver 13
   4.4 Summary of Terminal Characteristics 14

5. FIELD TRIAL RESULTS 15
   5.1 Introduction 15
   5.2 Ottawa Area Trials 15
   5.3 Resolute Bay Trials 17
   5.4 Churchill Trials 19
   5.5 Watson Lake Trials 21
   5.6 Frobisher Bay Trials 23
   5.7 Inuvik Trials 26

6. CONCLUSIONS 26
   6.1 Present System 26
   6.2 Further Work Required 27

7. REFERENCES 28

8. ACKNOWLEDGEMENTS 28

APPENDIX A - Atmospheric Noise Level Predictions 30

APPENDIX B - Parameters of a Dipole Antenna Lying on the Surface of the Earth 32

APPENDIX C - Low Frequency Solid State Transmitter 39

APPENDIX D - Low Frequency Receiver Circuit Description and Performance Characteristics 55

A TRANSPORTABLE LOW FREQUENCY COMMUNICATIONS SYSTEM

by

W.M. Evans

ABSTRACT

This report describes a highly portable, short-range, low-information-rate communications system and its associated electronics intended for use in the Canadian Arctic as a back-up to conventional HF systems. This low frequency system operates in the 100 kHz to 200 kHz band and employs an all solid-state transceiver capable of providing an output power in excess of 300 watts. The transmitting antenna is a 2000 foot dipole lying on the surface of the earth. One complete terminal for the system occupies about one cubic foot and weighs less than 50 pounds.

Results of several trials conducted in the Canadian Arctic at widespread locations are given and it is shown that a range of at least 200 miles has been achieved in all cases. Expected variations in the maximum communications range are examined in view of the effects of ground conductivity on the antenna efficiency and atmospheric noise on system sensitivity.

1. INTRODUCTION

1.1 REQUIREMENTS

The increasing interest in the Canadian north is resulting in requirements for specialized communications systems capable of providing specified services regardless of the environment encountered. Often human lives are dependent upon the reliability of a certain communications system. The point-to-point circuits presently employed use combinations of systems such as LF,

HF, and Tropospheric Scatter to provide the necessary reliability. If one system fails there is usually a different system available for emergency use.

The mobile communications systems presently available fall into two categories: HF and VHF systems. The HF systems can be used for short-, medium- or long-range communications, but lack the necessary reliability because of the effects that ionospheric disturbances have on the propagation of the HF skywave. The VHF systems have a very high reliability, but are limited to short-range use. Consequently, most vehicles in an arctic community are equipped with VHF radios and contact is kept with a central area or base station.

It is becoming more common these days for vehicles to undertake cross-country journeys of several hundred miles. For these vehicles, an HF communications system is necessary, but, as mentioned above, the arctic is subjected to a larger number of ionospheric disturbances than lower latitudes, and HF black-out can occur for periods of several days. Therefore, a definite requirement exists for an emergency communications system that can be used to establish reliable communications when the normal HF link is unusable.

One major characteristic of the emergency system must be its utilization of a propagation mechanism which is relatively unaffected by the ionospheric disturbances which cause degradations in HF communications. Because the system is to be used as a back-up, it must be as small and as light as possible so that it can be stowed away conveniently. The system must be capable of quick and easy deployment and must operate from existing power sources in a vehicle. Naturally, the electronics must be capable of normal operation at temperatures as low as -50°C.

A study of the location of communities in Northern Canada shows that there are very few places in the north that are more than 200 miles from at least one of these communities. This establishes a maximum range requirement of 200 miles for the emergency system.

1.2 POSSIBLE SOLUTIONS

The present rate of progress in providing higher power VHF and UHF communication satellites means that a simple, man-portable ground terminal will soon be all that is required for access. Such a satellite communications system is theoretically ideal, but the practical problems of controlling access, providing sufficient capacity and obtaining the required frequency allocations argue against such a system for the situation considered here.

It is possible to produce a very compact, light-weight and low-power VHF tropospheric scatter communications system that could provide the service required. Some practical problems are encountered because of the antenna alignment accuracies required. A separate CRC report on the tropospheric system designed for this application will be available soon.

The use of the low frequency ground wave as the propagation mechanism is a third way of providing a signal free from ionospheric effects. There are many problems to overcome in developing a portable LF communications system. These problems are considered in this report which provides the design of an LF system suitable for use in a mobile role, or as a point-to-point short-range system in the arctic.

1.3 PORTABLE LF ARCTIC COMMUNICATION SYSTEM

The equipment proposed for this system weighs approximately 50 pounds and occupies slightly more than one cubic foot of space, excluding the vehicle battery required as primary power source. The system electronics are completely solid-state, employing a very efficient class D amplifier to provide up to 400 watts of RF power to the transmitting antenna. The transmitting antenna is 2000 feet of insulated wire lying on the surface of the earth and can be deployed manually in less than 10 minutes. The receiver uses a 39 inch diameter loop antenna.

The system exploits the unique combination of low ground conductivity and low atmospheric noise level that are prevalent in the arctic. These characteristics are, however, seasonably and geographically variable and thus the system performance is similarly variable.

This report will discuss:

(a) the system design employed for the mobile situations;

(b) the characteristics of the transmitting antenna;

(c) the experimental results from various tests conducted near Ottawa and in the arctic; and

(d) the electronics employed in a laboratory model of a transceiver built to demonstrate the feasibility of the system.

2. LOW FREQUENCY SYSTEM DESIGN

2.1 INTRODUCTION

The following assumptions are made concerning the operational requirements:

(a) the maximum range required is 200 miles;

(b) 12 words per minute (wpm) Morse code modulation is sufficient but 60 wpm frequency shift keyed (FSK) teletype would be desirable;

(c) a 10 per cent word error rate is acceptable;

(d) the area of operation is the Canadian Arctic in regions of permafrost; and

(e) the equipment must be as small and light as possible, and be very easy to set up.

2.2 REQUIRED RMS CARRIER/RMS NOISE

Watt, *et al*[1], have performed an extensive series of tests to evaluate the performance of various communication systems in the presence of atmospheric noise, and the results of their work will be used here. The following assumptions are made:

(a) a Morse code operator of average ability is being used for the Morse code system; or

(b) a ± 25 Hz frequency shift keyed (FSK) teletype is used; and

(c) the receiver IF bandwidth is 100 Hz.

The atmospheric noise encountered during the trials reported in reference 1 had a dynamic range of 68 dB in a 1 kHz bandwidth. From the curves given in the paper, it appears that this would correspond to a dynamic range of about 55 dB in a 100 Hz bandwidth. When the data given for a one kHz bandwidth are converted to a 100 Hz bandwidth it is found that the following $\frac{\text{rms carrier}}{\text{rms noise}}$ levels are required:

12 wpm Morse code ..... + 7 dB

60 wpm FSK ..... +10 dB.

2.3 ATMOSPHERIC NOISE

The background noise in the 100-200 kHz band of interest is usually atmospheric. This noise is the result of thunderstorm activity around the world and is thus impulsive and has a magnitude that varies with latitude, time of day, and time of year. Fortunately, for this system application, the noise is considerably lower during periods of HF blackout.

The CCIR publishes atmospheric noise level predictions[2] which are used in Appendix A to calculate noise levels for the Arctic and the Ottawa area. Table 1 summarizes these results. The noise levels are the upper 90 per cent levels, or, in other words, the noise will be below the stated level for 90 per cent of the time during this period.

TABLE 1

Noise Level (dB > 1 μV/m)

Condition	Frequency	
	100 kHz	200 kHz
Maximum noise conditions in the Arctic (summer)	+ 14.3	+ 11.0
Minimum noise conditions in the Arctic (winter)	+ 4.5	- 7.5

2.4 MAN-MADE NOISE

At many locations in the north electrical power distribution systems can cause electrostatic fields which produce, in unshielded antennas, noise levels considerably higher than the atmospheric noise. Motor vehicles can cause the same condition. To ensure that this type of noise does not adversely affect the system performance, an electrostatically shielded magnetic dipole antenna (loop antenna) is used for the receiver antenna. This antenna has proven very successful in all the field trials and at no time was man-made noise a factor in limiting the system performance.

2.5 REQUIRED SIGNAL LEVELS AT RECEIVER TERMINAL

According to the statistics shown in reference 1, the upper decile level of the noise distribution is very close to the rms value and thus the levels quoted in Appendix A will be used here as the rms values of the noise. This fact is basically a result of the large dynamic range of the atmospheric noise. These noise levels (in dB > 1 μV/m) are added to the required rms carrier/rms noise. Table 2 summarizes the resultant required signal levels.

TABLE 2

Required Signal Level (dB > 1 μV/m)

Condition	Frequency			
	100 kHz		200 kHz	
	Morse Code	FSK	Morse Code	FSK
Maximum noise in Arctic	21.3	24.3	11.5	14.5
Minimum noise in Arctic	18.0	21.0	-0.5	2.5

The many trials conducted in the north have indicated that, in the winter, the atmospheric noise is often considerably below the predicted values calculated in Appendix A and is often below the receiver system sensitivity. As is shown in Section 4.3, this sensitivity is 15 dB below one microvolt/meter at 100 kHz and 21 dB below one microvolt/meter at 200 kHz. When the atmospheric noise is below the system sensitivity the following signal levels are required.

TABLE 3

Required Signal Level (dB > 1 μV/m)

Condition	Frequency			
	100 kHz		200 kHz	
	Morse Code	FSK	Morse Code	FSK
Thermal noise	-8	-5	-14	-11

2.6 GROUND WAVE PROPAGATION ATTENUATION

The attenuation-vs-distance characteristics of the low frequency ground wave can be predicted accurately if the conductivity of the ground path is known. Figure 1 shows the theoretical attenuation curves for four ground conductivities and a frequency of 100 kHz. The curves clearly show the increased attenuation caused by decreasing ground conductivity. This attenuation is also a function of frequency and Figure 2 plots the relative attenuation at a distance of 200 miles for the same four conductivities. These curves indicate that there should be considerable advantage in using an operating frequency near 100 kHz, but when the inverse-frequency dependence of the atmospheric noise is considered, this advantage largely disappears.

Table 4 summarizes the attenuations to be expected when the receiver is located 200 miles from the transmitter.

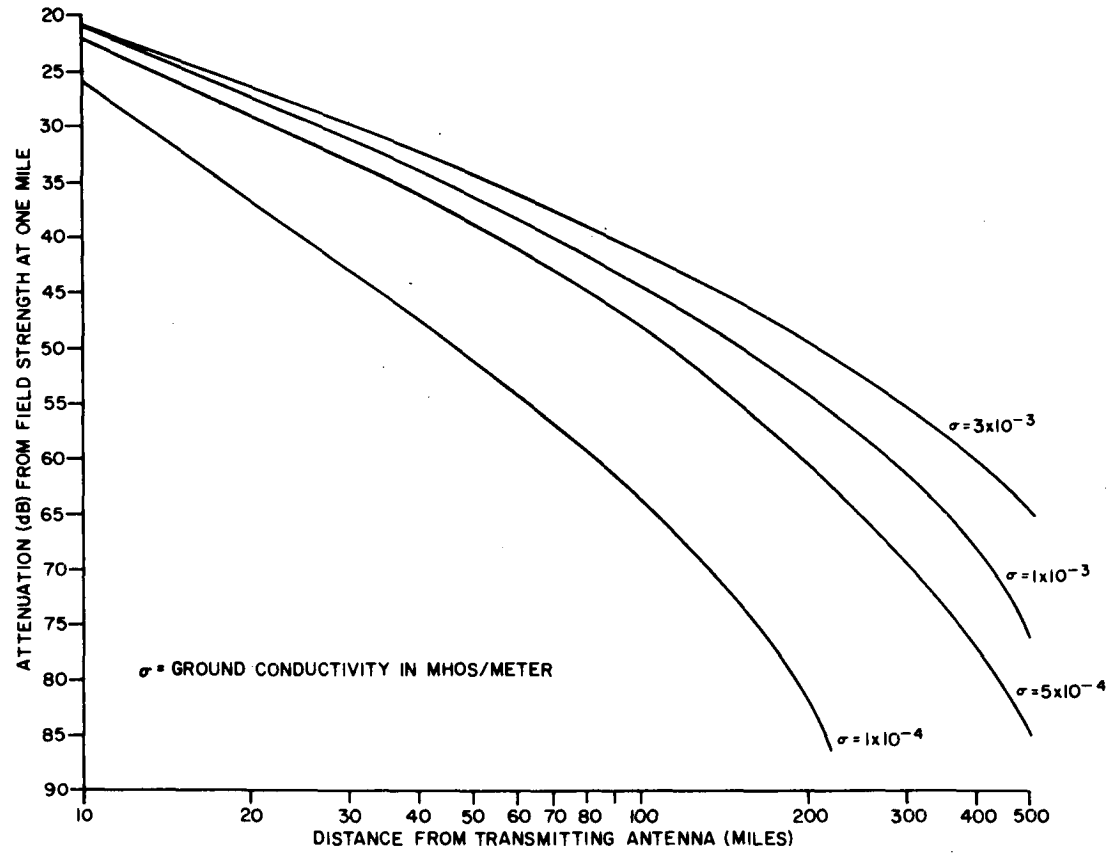

Fig. 1. Ground wave attenuation characteristics for a frequency of 100 kHz.

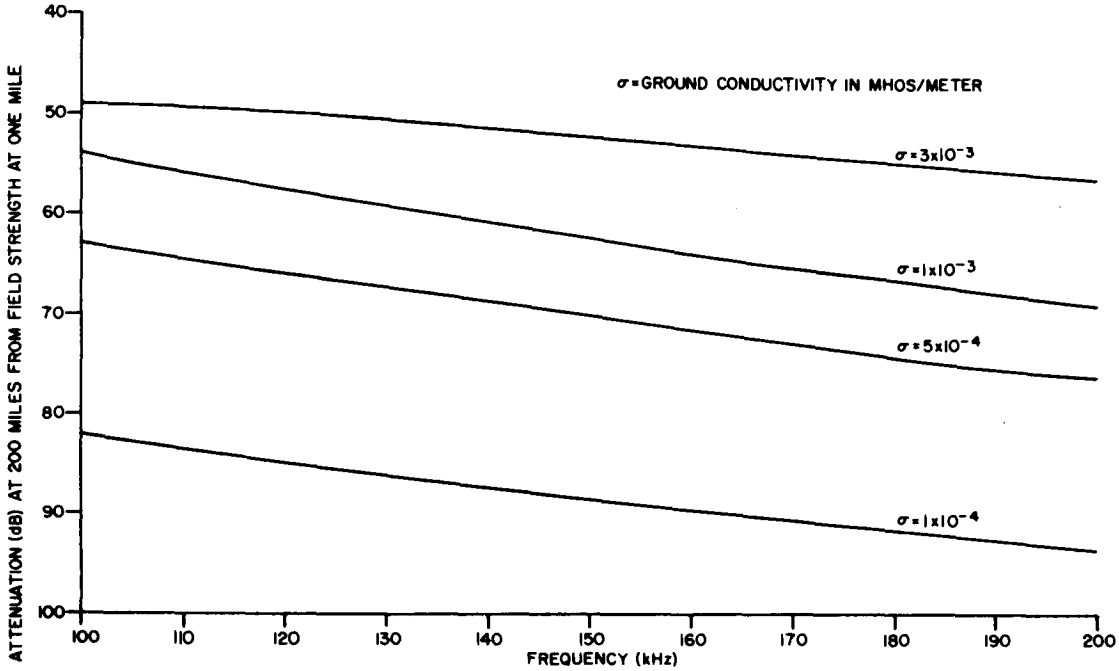

Fig. 2. Ground wave attenuation at a distance of 200 miles from the transmitter.

TABLE 4

Propagation Attenuation at 200 Miles

(dB relative to signal at one mile)

Ground Conductivity (mhos/meter)	Frequency	
	100 kHz	200 kHz
3×10^{-3}	49	57
1×10^{-3}	54	69
5×10^{-4}	63	77
1×10^{-4}	82	94

2.7 REQUIRED RADIATED POWER

By adding the attenuation figures to the required signal level figures the required signal strength at a distance of one mile from the transmitter is obtained. Norton[3] states that the vertical component of electric field strength at a distance of one mile from a $\lambda/4$ vertical monopole is equal to 97.3 millivolts per meter (mV/m) when one kilowatt of power is radiated. In other words

$$E = 97.3 \times (P_r)^{\frac{1}{2}}$$

where E = vertical component of field strength at one mile (mV/m)

and P_r = radiated power in kilowatts.

Manipulation of this equation yields

$$P_r = \frac{(E)^2}{9467} .$$

Substituting the required values for E, the required radiated power is calculated and Table 5 summarizes the results. The lower power value in each square is for a ground conductivity of 3×10^{-3} mhos/meter while the high value is for a conductivity of 1×10^{-4} mhos/meter. For a perfect omnidirectional antenna with no losses, the required radiated power is also the transmitter output power. For a realizable antenna, the transmitter power can be obtained by multiplying the required radiated power by the inverse of the fractional efficiency of the antenna.

TABLE 5

Required Radiated Power (watts) for a Range of 200 Miles

	Frequency			
	100 kHz		200 kHz	
Background Noise	Morse Code	FSK	Morse Code	FSK
Maximum atmospheric noise in Arctic	1.13-1337	2.26-2674	.47-3733	.94-7473
Minimum atmospheric noise in Arctic	0.53-1056	1.05-2100	.047-236	.094-474
Thermal noise	1.33×10^{-3}-2.6	2.6×10^{-3}	1.05×10^{-3}	4.0×10^{-3}

It is obvious from these figures that a system designed to meet the worst case (FSK at 200 kHz with maximum atmospheric noise and a ground conductivity of 1×10^{-4} mhos/meter) would require a radiated power about 70 dB above the power required for the best case (Morse code at 200 kHz with thermal noise and a ground conductivity of 3×10^{-3} mhos/meter). Fortunately, this system is intended for emergency use when ionospheric disturbances have caused HF blackout and it is at these times that the atmospheric noise levels are lowest. Experience in the field has shown that during the winter months and at 200 kHz the atmospheric noise is generally below the receive system sensitivity. Therefore, the figures of importance from the previous table are the powers required to provide FSK communications at 200 kHz with thermal noise limiting the receiver sensitivity. If the conductivity is 1×10^{-4} mhos/meter, 42 watts of radiated power are required and if the conductivity is 3×10^{-3} mhos/meter only four milliwatts of radiated power are required.

2.8 SUMMARY OF SYSTEM DESIGN

The previous paragraphs have outlined the signal level requirements for a wide variety of conditions that could prevail in the Canadian Arctic. It is clear that a system designed for use at the highest noise levels would have to use very high powers (radiated power greater than 7000 watts), and would require very large and expensive electronics and power supplies. Since this system is designed for emergency use only, it must be small and light and operate from existing power supplies. As mentioned before, these emergency conditions would generally occur in the winter during periods of HF blackout, and it is during this time that the atmospheric noise is minimized. In fact, limited experience in the field suggests this noise will be below the thermal noise of a very sensitive receiver. It follows that maximizing receiving system sensitivity is a desirable goal in system design. This is probably not a surprising statement, but it indicates a departure from normal low frequency systems designed for use in the presence of high level atmospheric noise.

The required radiated power analysis has shown that there are two variables (ground conductivity and background noise level) which are not under the control of the system user and these variables can cause a wide variation in communications ranges for a given transmitter power. It was decided that the highest possible transmitter power, consistent with normal vehicle power supplies, should be provided. It is also apparent that maximizing the efficiency of converting the dc power to RF power is an essential design criterion since the whole system would be limited by available dc power.

All of the above design criteria formed the basis for the system philosophy. The following section will describe in more detail the actual parameters embodied in the experimental system built for demonstration purposes.

3. TRANSMITTING ANTENNA

3.1 INTRODUCTION

An antenna system was required which was compact, light, and quickly deployable and recoverable in arctic conditions. The simplest antenna that meets the above requirements is a dipole lying on the surface of the earth. It requires no supports, no masts, no ground system and is light and compact when rolled up. The low ground conductivity prevailing in most of the arctic will improve the radiation characteristics of this type of antenna, instead of impairing it as it does for the normal vertical antenna.

The ground conductivities at a frequency of 10 kHz for most of the area of concern have been determined by Maxwell and Morgan[4] to be approximately one order of magnitude less than that in the Ottawa area. This results in reduced ground losses in the vicinity of the horizontal antenna and better radiation, while increasing the ground loss associated with vertical antennas. The arctic terrain is mostly open and flat so that space and deployment would be no problem for the horizontal antenna. These arctic characteristics and the work done elsewhere[5] on horizontal antennas at LF encouraged the idea of investigating the use of a $\lambda/2$ dipole lying on the ground for the portable LF system. The theoretical and experimental determination of the antenna parameters are discussed in Appendix B.

3.2 TRANSMITTING ANTENNA CHARACTERISTICS

The antenna used during the field trials has the following characteristics:

length	2000 feet
gauge	AWG 18
stranding	19 x 30
insulation	teflon covered, 1000 volt
operating temperature range	-60°C to +100°C
manufacturer	Beldon type 83029.

This wire was selected because the excellent low temperature performance of the teflon insulation allows frequent deployment and retrieval in very cold temperatures without damage to the insulation. The antenna was wound onto two standard military cable reels (1000 feet on each). These reels were then used in a military, hand-operated, cable winding machine. Figure 3 shows an operator retrieving one leg of the antenna. The antenna system, complete with winding machines, weighs about 25 pounds.

As shown in Appendix B, the radiation pattern of this type of antenna is a figure eight with maximum radiation along the axis of the antenna. This means that the antenna must be pointed in the direction of the distant terminal.

The efficiency of the antenna is variable and Appendix B indicates that the expected worst case efficiency is about 0.1 per cent (-30 dB). In other words, if the transmitter feeds 350 watts to the antenna, only 350 milliwatts

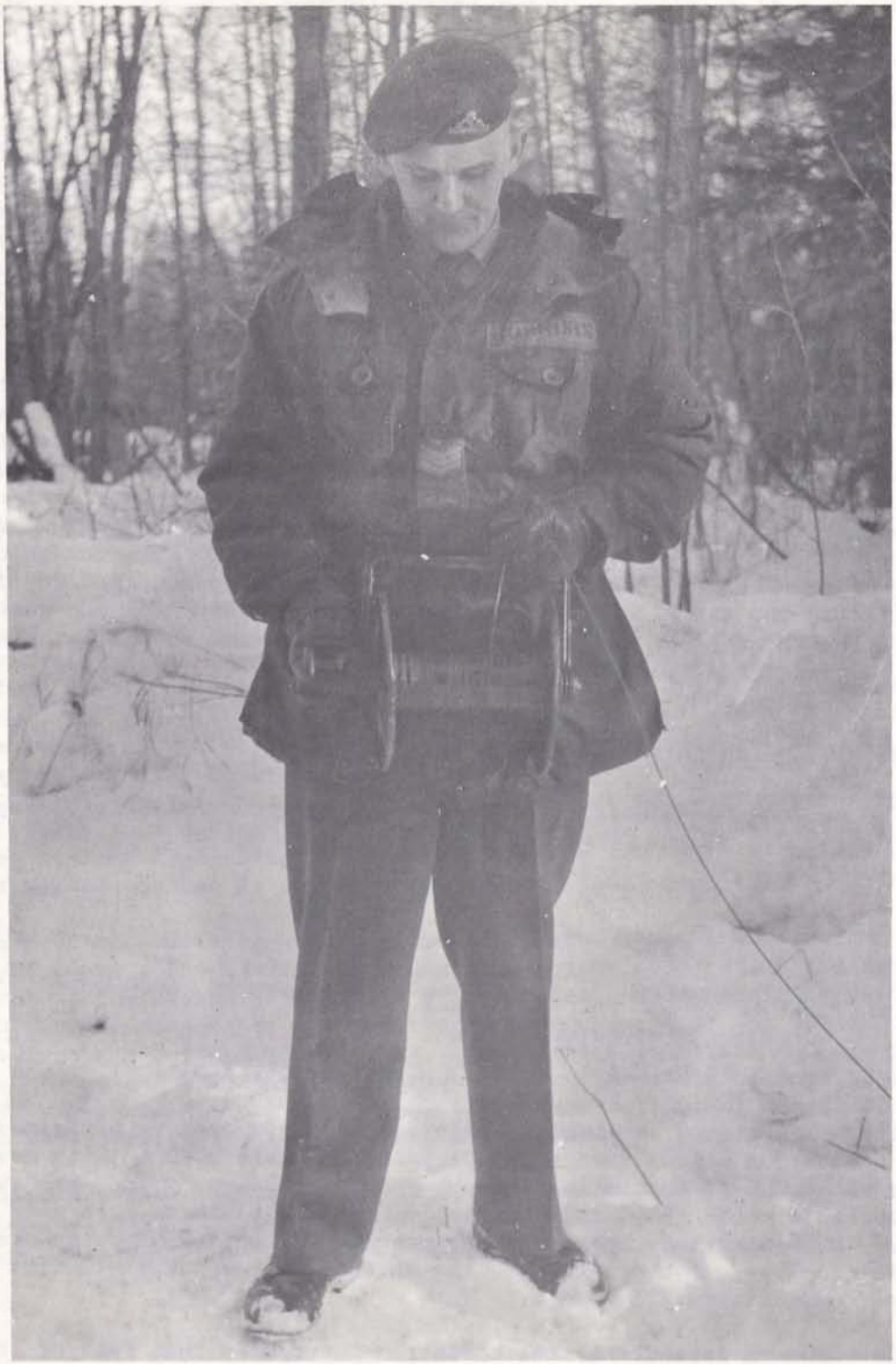

Fig. 3. Transmitting antenna retrieval.

are radiated. This indicates clearly the problem of most low frequency communications systems--the relatively poor efficiency of the transmitting antenna systems. Only large elaborate systems employing extensive counterpoises and top loading can improve the efficiency significantly.

4. COMMUNICATIONS TERMINAL DESCRIPTION

4.1 INTRODUCTION

Two Morse code transceivers were constructed for system demonstration purposes. Figure 4 shows one of these transceivers. The dimensions of the unit are 19" x 8" x 8" and it weighs 25 pounds. The receiver occupies the left hand third of the set while the remainder of the space is occupied by the transmitter. The six output transistors are shown in the heat sink along the right hand side.

This transceiver represents a compromise between an operational and a scientific unit. The large meters and some of the controls would not be necessary for an operational unit. The set has been designed to be protected from mis-tuned operation, reverse polarity battery connection, short or open circuit antenna connections, and overheating of the power amplifier devices. Should any of these faults occur, the power amplifier is turned off before damage can occur and the 'overload' indicators flash on and off. The 'reset' button is activated after the fault has been corrected and the transmitter can be operated again.

4.2 LOW FREQUENCY SOLID-STATE TRANSMITTER

The recent advances in solid-state devices have permitted the application of class D amplifiers to relatively high-powered low frequency transmitters. The class D amplifier forms the basis of the transmitter section of the transceiver and Appendix C gives a detailed description of the electronic circuits employed.

Table 6 summarizes the characteristics of the transmitter.

TABLE 6

Transmitter Characteristics

Frequency range	3 crystal controlled channels between 100 and 200 kHz
Frequency stability	± 5 Hz over temperature range - 40°C to + 80°C
Output power	Nominally 350 watts
Harmonics output	More than 30 dB below the carrier

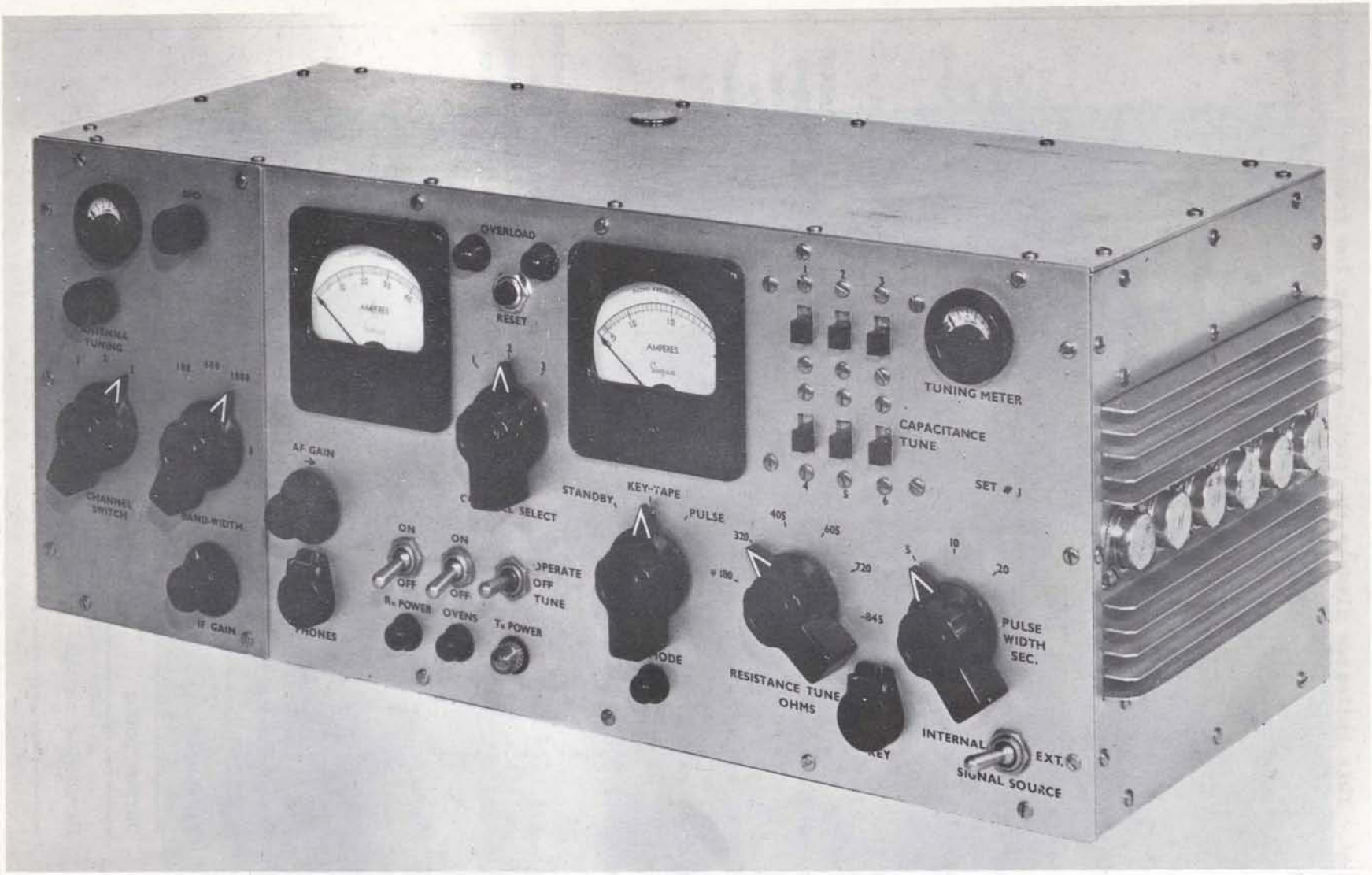

Fig. 4. Low frequency solid state transceiver.

TABLE 6 (Cont'd)

Transmitter Characteristics

DC to RF efficiency	70%
Antenna tuning unit	Can match antennas with input parallel resistances varying from 100 to 1000 ohms and input parallel reactances from +300 ohms to -600 ohms.
Modulation	Morse code: either hand-keyed or from a magnetic tape recorder; or an internally generated series of pulses.
Input voltage range	18 to 30 VDC

4.3 LF SOLID-STATE RECEIVER

The receiver employs dual conversion and is designed for the reception of the Morse code. A low-noise preamplifier is used to allow the system to take advantage of the low atmospheric noise levels prevalent in the arctic. A tuned, electrostatically shielded loop antenna is used in order to reduce man-made interference.

The detailed design and performance characteristics of the receiver are presented in Appendix D.

Table 7 lists the specifications for the LF receiver:

TABLE 7

Receiver Characteristics

Sensitivity	15 dB<1μV/meter at 100 kHz 21 dB<1μV/meter at 200 kHz
Noise figure	3 dB
3 dB bandwidth	selectable - 100 Hz - 500 Hz - 2000 Hz
Frequency stability	±5 Hz from -35°C to +10°C
Dynamic range	90 dB
Channels	3 crystal controlled between 100 and 200 kHz
Input	balanced
Outputs	high impedance and 600 ohms

4.4 SUMMARY OF TERMINAL CHARACTERISTICS

Figure 5 shows one complete communications terminal, including the 24 volt lead-acid battery supply. Two of these terminals were constructed for demonstration purposes and were used in trials at Churchill Manitoba, Watson Lake in the Yukon, and Frobisher Bay on Baffin Island. In building the complete terminal, time did not allow for miniaturization of the electronics and the construction of a collapsible loop antenna. It is felt that state-of-the-art circuit and packaging techniques would considerably reduce the size and weight of the terminal.

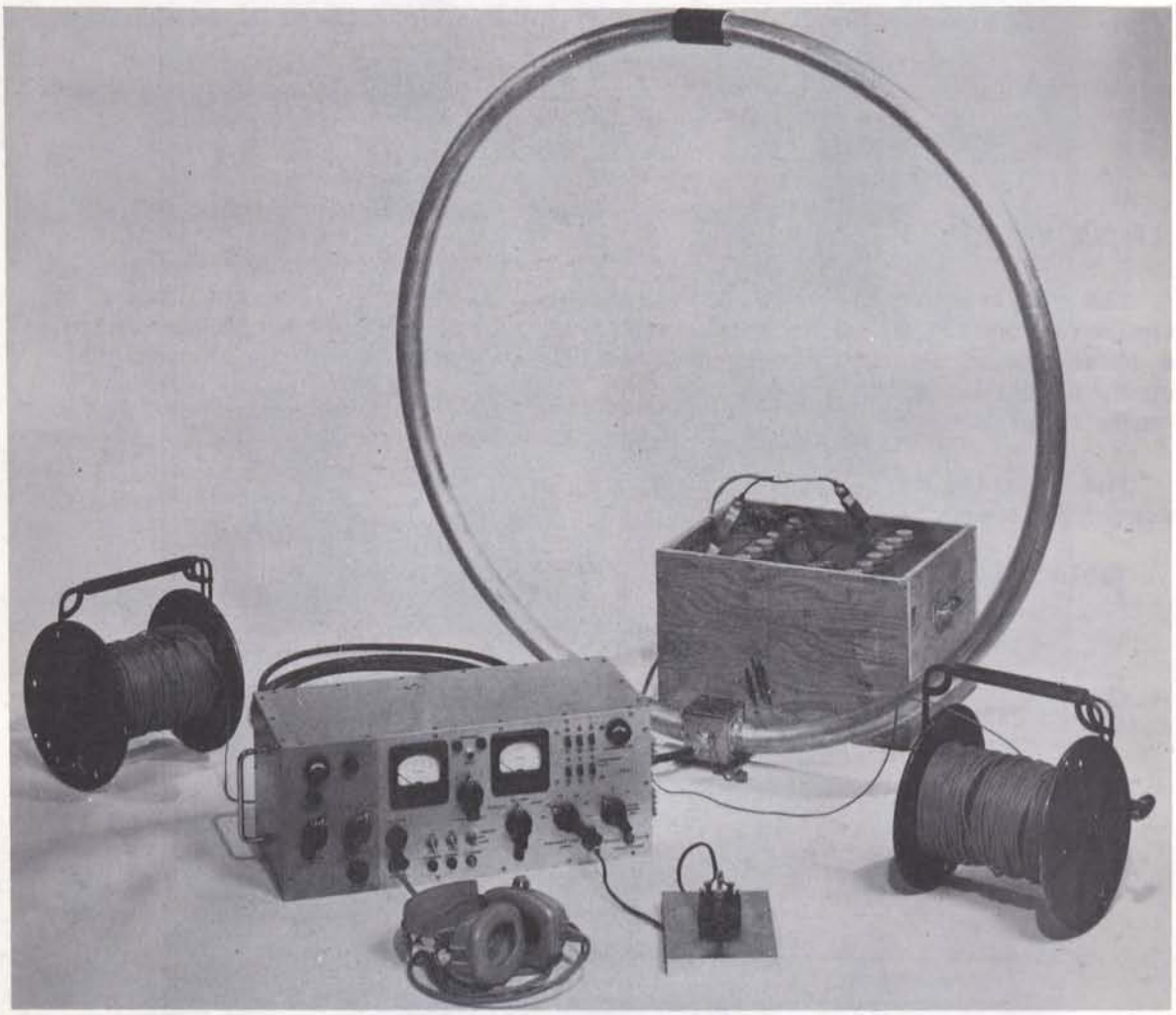

Fig. 5. Low frequency communications terminal.

Table 8 summarizes the characteristics of the communications terminal.

TABLE 8

Communications Terminal Characteristics

Total terminal weight (excluding power supply)	less than 50 lbs.
Transceiver	size - 19" x 8" x 8" weight - 25 lbs, power supply - external vehicle battery, 24 volts
Frequencies	channel 1 - 110.75 kHz channel 2 - 141.00 kHz channel 3 - 171.00 kHz
Transmitting antenna	2000 feet of AWG 18 teflon insulated wire
Receiving antenna	39" diameter loop antenna
Transmitter output power	nominally 350 watts
Receiving system sensitivity	15 dB below one microvolt per meter at 100 kHz 21 dB below one microvolt per meter at 200 kHz
Modulation technique	hand keyed Morse code

5. FIELD TRIAL RESULTS

5.1 INTRODUCTION

The entire communications system has been tested in many areas of Canada. Figure 6 shows the locations of the communications trials and indicates those links which gave successful performance and the two links which were not successful. The Resolute Bay trials did not use the equipment described in this report, but used a similar transmitter and a specially modified field intensity meter as a receiver.

5.2 OTTAWA AREA TRIALS

The majority of the preliminary experimental work to establish the various system parameters was done in the Ottawa area. Antenna impedance measurements were made during most of the significant weather conditions prevalent in this area. One effect of weather on the antenna impedance is simply to shift the resonant frequency from about 110 kHz on a very wet day to 150 kHz on very dry days. This is not a serious effect, but it does mean that the transmitter must be retuned if the moisture content of the ground changes.

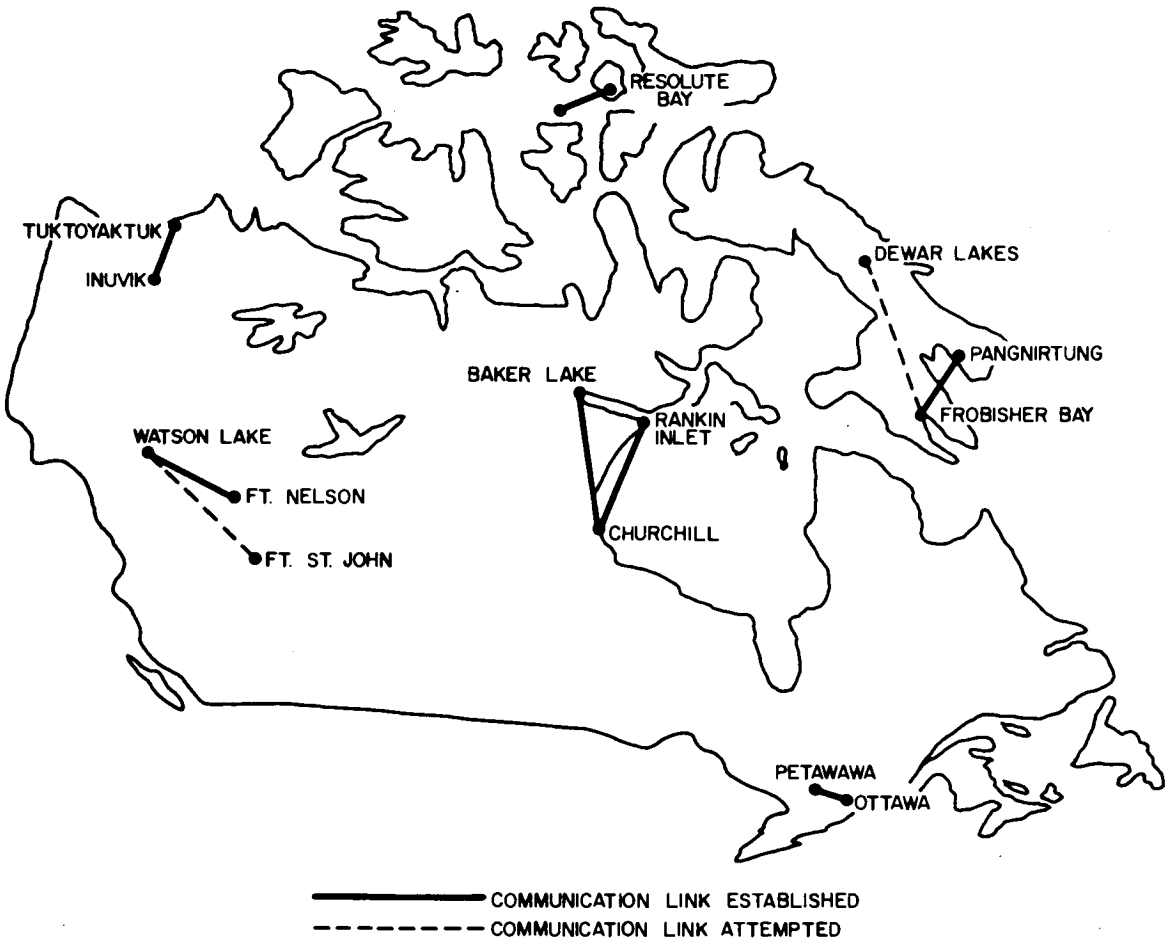

Fig. 6. Communications field trials site locations.

Of a more serious nature is the effect of ground moisture on the antenna efficiency and therefore on the communications range. Figure 7 shows two measured field strength-versus-distance curves for the same antenna located in the same place but with the ground very dry for the top curve and very wet for the bottom curve. The efficiency is a result of field strength measurements at one mile and is stated in terms of dB relative to a perfect quarter-wave vertical antenna. It is obvious that the 14 dB loss in efficiency caused by the very wet ground will result in a major reduction in system performance.

One-way communications trials using the terminals described were conducted in January 1969. The transmitting terminal was located at Shirley Bay, just to the west of Ottawa and the receiving terminal was driven along Highway 17 towards Petawawa. Field intensity measurements were not made, but the audio output of the receiver was recorded on magnetic tape. This magnetic tape was later played back for subjective quality estimates by a Morse code operator. The information on the tape was transferred to a high-speed chart recorder to facilitate analysis.

At Petawawa a distance of 80 miles from the transmitter and at a frequency of 171 kHz the peaks of the atmospheric noise at 1700 hours local time, were just strong enough to obliterate a character occasionally and a 4 per cent

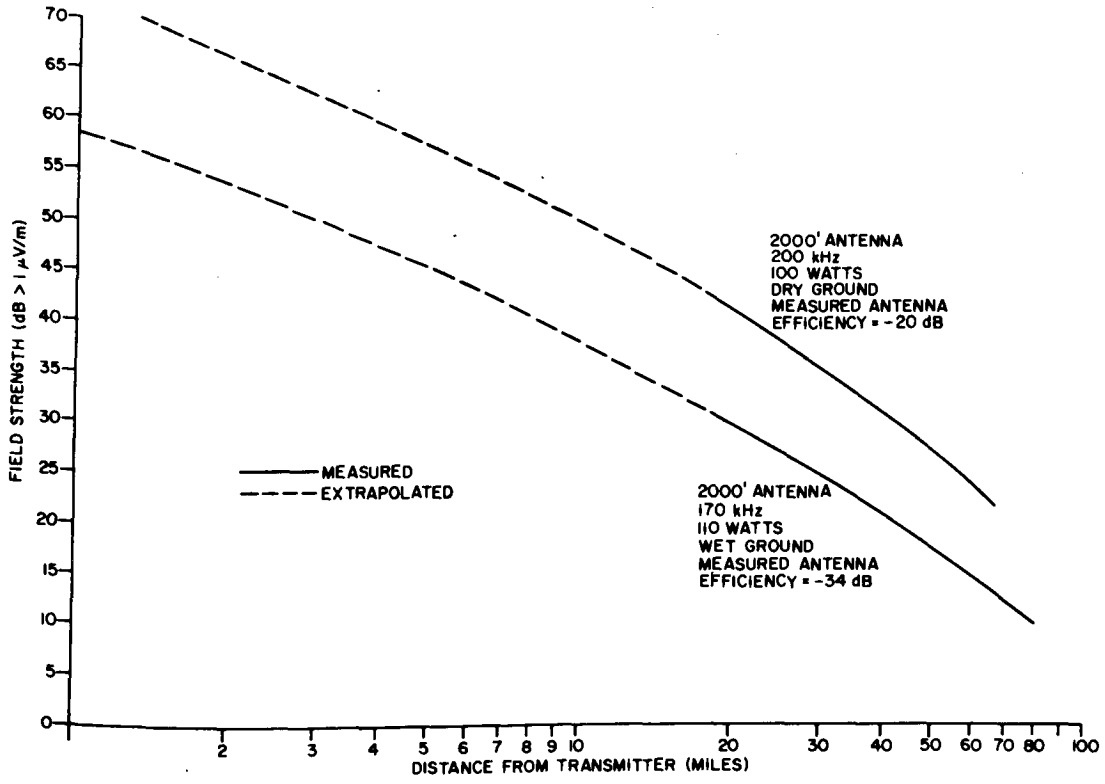

Fig. 7. Field strength attenuation curves measured near Ottawa.

character error rate was achieved. Figure 8(a) shows the chart recording of this signal when no atmospheric noise bursts are present while Figure 8(b) shows another part of the recording with an atmospheric noise burst. The average signal-to-noise ratio is about 21 dB, but when the noise burst occurs the intelligence is obscured to the ear.

5.3 RESOLUTE BAY TRIALS

These trials took place in May 1968 and were basically designed to obtain the parameters of the transmitting antenna and only a short 100 mile communications test was conducted. The conditions were ideal for the system since the antenna was located on the low conductivity permafrost while the communications path was almost entirely over the high conductivity sea ice. This condition combined high antenna efficiency with low propagation attenuation. As a result, the signal strength was 27 dB>1μV/m at a distance of 100 miles (S/N = 45 dB).

The noise levels were at all times below the system sensitivity, and the communications range for these conditions would exceed 600 miles. If the propagation had been entirely over a land path with a conductivity of 5×10^{-4} mhos/meter, the communications range would have been reduced to about 350 miles.

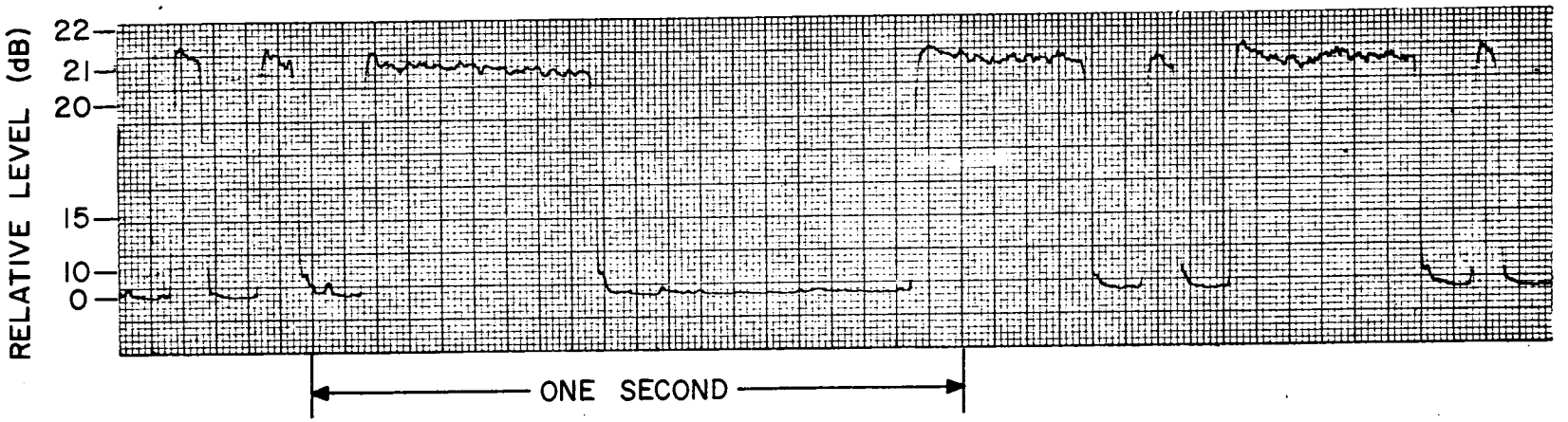

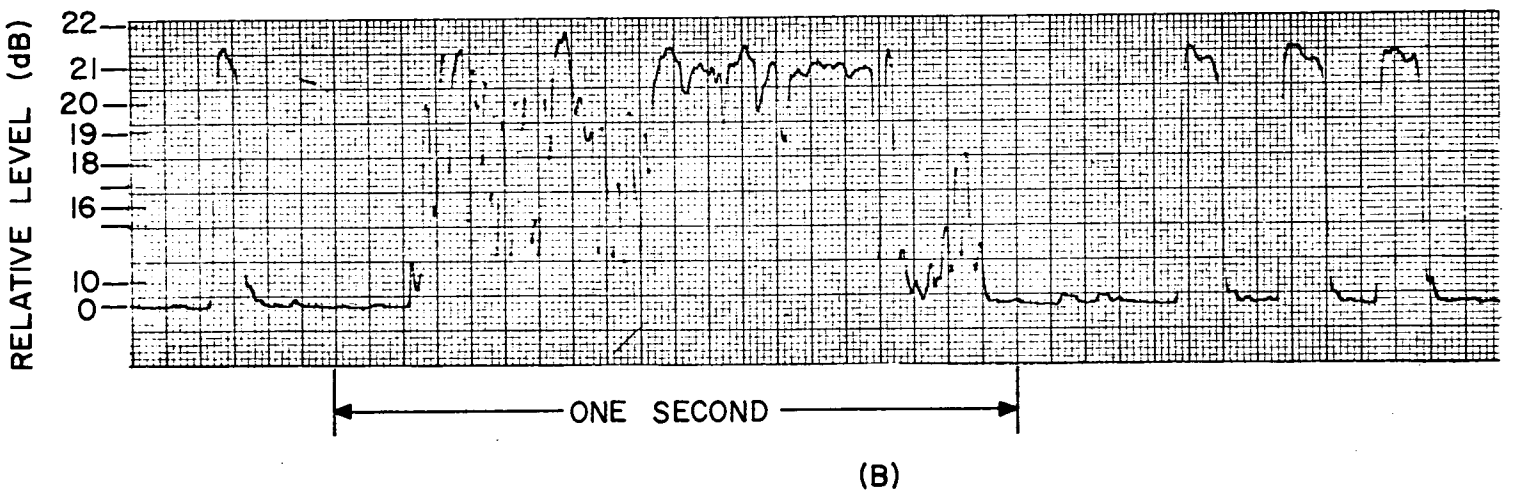

Fig. 8 Ottawa - Petawawa (80 miles) signals, January 1969, 1700 hours
(a) No atmospheric noise bursts

5.4 CHURCHILL TRIALS

The first northern trials of the complete system and the communications terminals as described in Section 4 were undertaken in January 1969 between Churchill, Manitoba and Rankin Inlet, N.W.T. and between Churchill and Baker Lake, N.W.T. These two paths are shown in Figure 6.

The weather during the tests was extremely cold with day-time temperatures of -40°F and winds up to 25 mph. Both transmitter and receiver performed well at these temperatures although the overall dc to RF efficiency of the transmitter often dropped to about 50 per cent.

Because of logistic problems, only one-way communications were tried, with the Churchill terminal doing the transmitting. The transmitting antenna was deployed just west of the Radar Site and on top of hard packed snow. The center of the antenna was about one mile from the shores of Hudson Bay. The input parallel resistance of the antenna is shown in Figure B - 4 of Appendix B.

The Churchill-to-Rankin Inlet path is 295 miles long, entirely over sea ice. A communications test was conducted between 1500 and 1600 hours local time on 28 January 1969. The transmitter was delivering 276 watts to the antenna and the received signal-to-noise ratio at Rankin Inlet was 28 dB. There were no large atmospheric noise bursts and no errors occurred in copying the twelve words-per-minute Morse code test transmissions.

The next day the terminal was transported from Rankin Inlet to Baker Lake and a communications test conducted between 1900 and 2000 hours local time. The first 125 miles of this 394 mile path are over sea ice, the remaining 269 miles are typical arctic tundra. The transmitter delivered 264 watts to the antenna and the average received signal-to-noise ratio was 21 dB, with atmospheric noise as the background. Again, this was sufficient for 100 per cent copy of the test transmissions. Figure 9(a) shows a chart recording of the signal.

The test was repeated the next day between 1100 and 1200 hours with 340 watts delivered to the antenna. This time the atmospheric noise level had subsided and the audio tape showed a signal-to-noise ratio of 29 dB. The chart recording for this signal is shown as Figure 9(b) and because only a range of 22 dB is shown, the background noise level is not visible. It is obvious that error-free copy of this signal was possible.

The conditions for this test were almost ideal and the results were very encouraging. The antenna was located on permafrost where it had good efficiency and the initial path was over the high conductivity sea ice where path attenuation was a minimum. The winter-time atmospheric noise level was very low and consequently the signal-to-noise ratio at 400 miles was very high.

It is possible to extrapolate the above results and predict communications ranges for an all land path similar to the land portion of the above path, all other variables remaining constant. Such an extrapolation yields a maximum communications range of 400 miles. From noise level prediction charts, a 20 dB increase in the noise level can be expected in the summer resulting in a maximum summer time range of 230 miles.

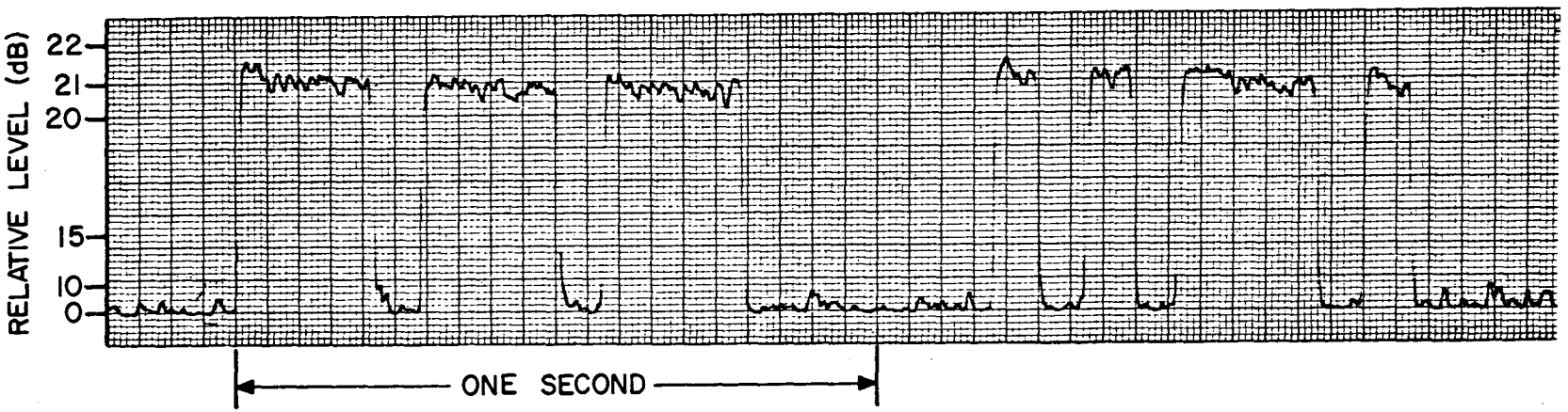

(A) 1900 HRS.

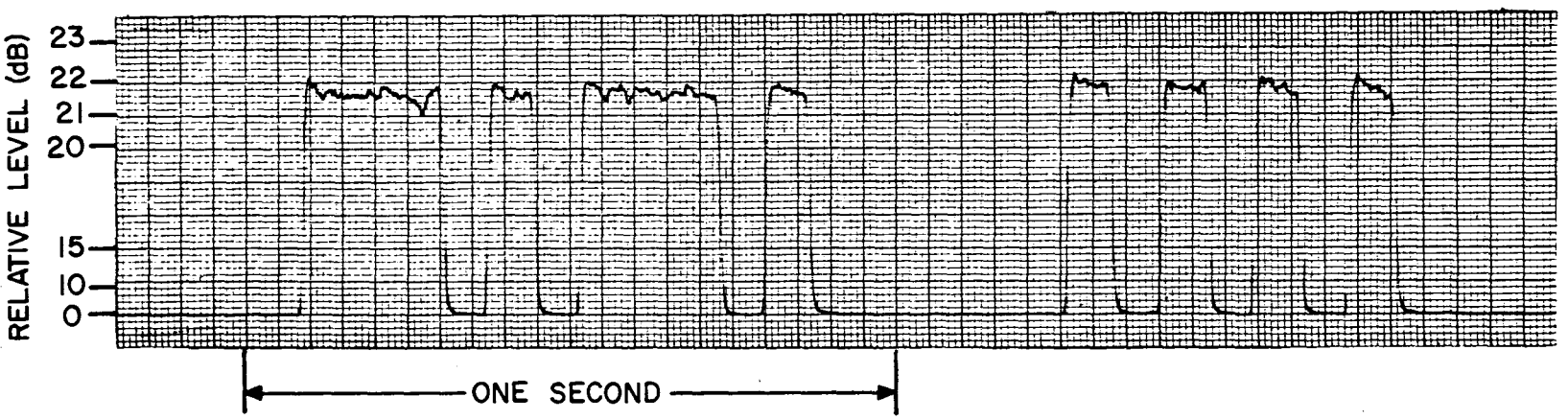

(B) 1100 HRS.

Fig. 9. Churchill - Baker Lake (394 miles) signals, January 1969.

5.5 WATSON LAKE TRIALS

During the period 9-14 March, 1969, the communications terminals were operated by members of the Canadian Airborne Regiment during exercise "Noble Reply". A two-way communications link was established between Watson Lake, N.W.T. and Ft. Nelson, B.C. (see Figure 6), a distance of 240 miles. During the latter part of the exercise, an attempt was made to establish communications between Watson Lake and Ft. St. John, a distance of 390 miles, but no signals were heard.

At Watson Lake the transmitting antenna was deployed beside a road cut into the forest, and rested on about five feet of soft melting snow. The terminal was 0.5 miles from the military headquarters and all its associated motor-generators, and about two miles from the airport low frequency beacon. At no time did the beacon or the military HF radio sets interfere with the LF set.

At Ft. Nelson, the antenna was deployed along a firebreak in the forest adjacent to the town. The ground was a mixture of slush and mud.

The path between the two sites was mostly heavily forested foothills and neither terminal was located in an area of permafrost. In fact, the area represented what is considered to be a very poor site for this communications system. The sites were not far enough north to take advantage of the permafrost and low atmospheric noise levels. However, the military signals operators rated the Watson Lake - Ft. Nelson link as Q4 to Q5 during the daytime and Q1 to Q3 during the night when the noise levels rose.

Analysis of the tape recordings yielded an average signal-to-noise ratio of about 10 dB during the daytime, falling to 3 dB at night time. The daytime signals were sufficient for good readability but copy was very difficult, and sometimes impossible, at night. Figure 10(a) is a chart recording of the signals at 1500 hours local time, while Figure 10(b) shows the signals received at 2000 hours. The latter recording indicates how marginal the link was at night.

These trials represented the first time the system and terminals had operated as a self-sufficient two-way communications link. Analysis of the recordings made at both receiver sites indicated that the performance was nearly identical. At both sites and at all times, the background noise was atmospheric and for this reason the maximum range was limited to about 250 miles. The summer range would be even less.

This trial was very important because it showed the limitations the geographical area can impose on the system performance. It is felt that two factors contributed greatly to the degradation of the maximum range of the system. The atmospheric noise levels were high and the ground upon which the antennas were laid was very moist, and as shown in Figure 7, this moisture can cause more than 10 dB loss in antenna efficiency.

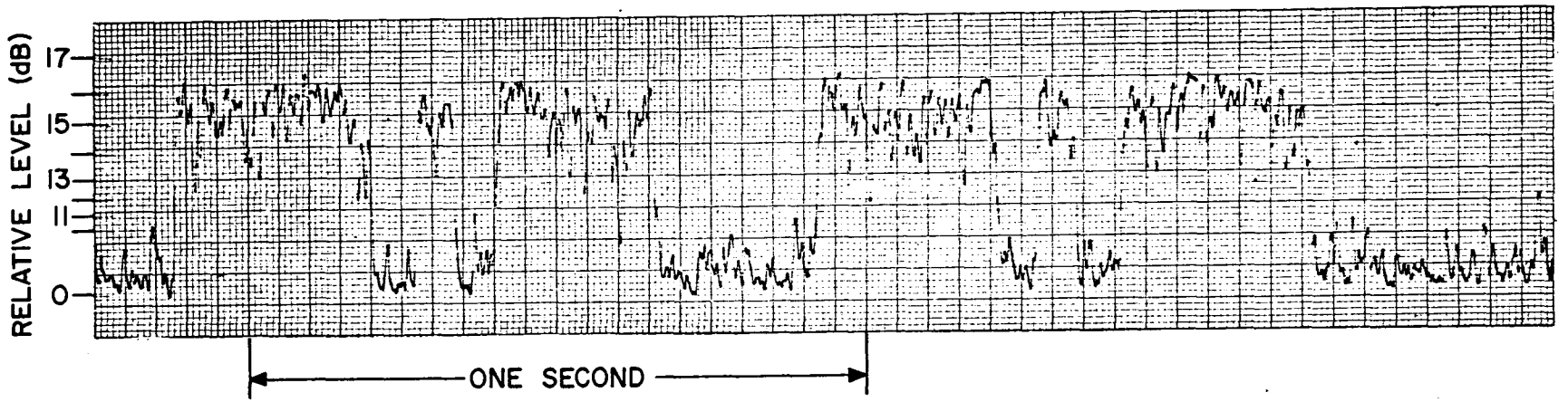

(A) 1500 HRS.

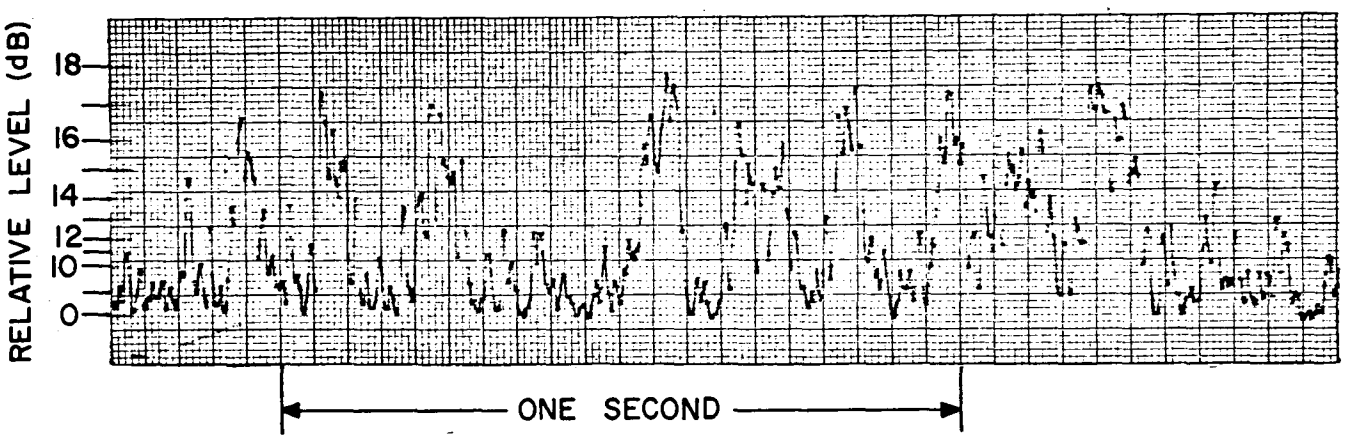

(B) 2000 HRS.

Fig. 10. Ft. Nelson - Watson Lake (240 miles) signals, March 1969.

5.6 FROBISHER BAY TRIALS

In order to evaluate further the geographical effects on system performance, a field trial was conducted on Baffin Island with the help of signallers from the Canadian Airborne Regiment during the period 20-27 August 1969. Since this was not a full scale military exercise, it was possible to make some scientific measurements of system parameters as well as to conduct communications tests.

The main camp was established at Frobisher Bay near the north-west corner of the main runway and the antenna was laid on a combination of soggy moss, sand, and rock out-croppings.

The first out-station was established at Pangnirtung, 188 miles away, with the antenna located on fairly dry moss.

After several days at Pangnirtung the terminal was transported to Dewar Lakes, 320 miles from Frobisher. The antenna was laid on very dry rocky ground at Dewar Lakes. The antenna input parallel resistances measured at the three sites are plotted in Figure 11. As can be seen, they are very similar to each other and to the Churchill resistances shown in Figure B-4 of Appendix B.

The efficiency of the antenna at Frobisher Bay was measured by taking field strength measurements at a distance of two miles. The antenna had an efficiency of -28 dB at a frequency of 171 kHz. Unfortunately the same measurements were not made at the other sites.

Two-way communications were established between Frobisher Bay and Pangnirtung on a regularly scheduled basis for three days. The signal strength at Pangnirtung was 24 dB>1 μV/m with 300 watts input to the antenna at Frobisher Bay, while the daytime noise level was about one microvolt per meter. This allowed 100 per cent copy by the military operators. A chart recording of this signal is shown in Figure 12(a). At night, the noise level rose to an average level of 15 dB>1 μV/m, still leaving sufficient average signal-to-noise ratio for copy with less than a 5 per cent character error rate. Figure 12(b) shows the chart recording of the signal and noise for 2230 hours local time.

Although the signals received at Pangnirtung were always sufficient to give less than 10 per cent word error rate, the signals received at Frobisher Bay were about 10 dB lower in level. This resulted in traffic loss at night at Frobisher Bay. This loss in system reciprocity is most likely a result of a different antenna efficiency, but this can not be proven since the efficiency was not measured at Pangnirtung.

The presence of sky-wave and ground-wave interference further complicated nocturnal operations at both sites. This was the only time in any of the field trials that the sky-wave signal was noticed. The fading rate was quite slow, of the order of two to five minutes, and the fading range was approximately 10 dB.

A one-day trial was attempted between Frobisher Bay and Dewar Lakes and no signals were heard at either site. The path was 300 miles long, entirely over very barren land, and had higher attenuation than the combination land-

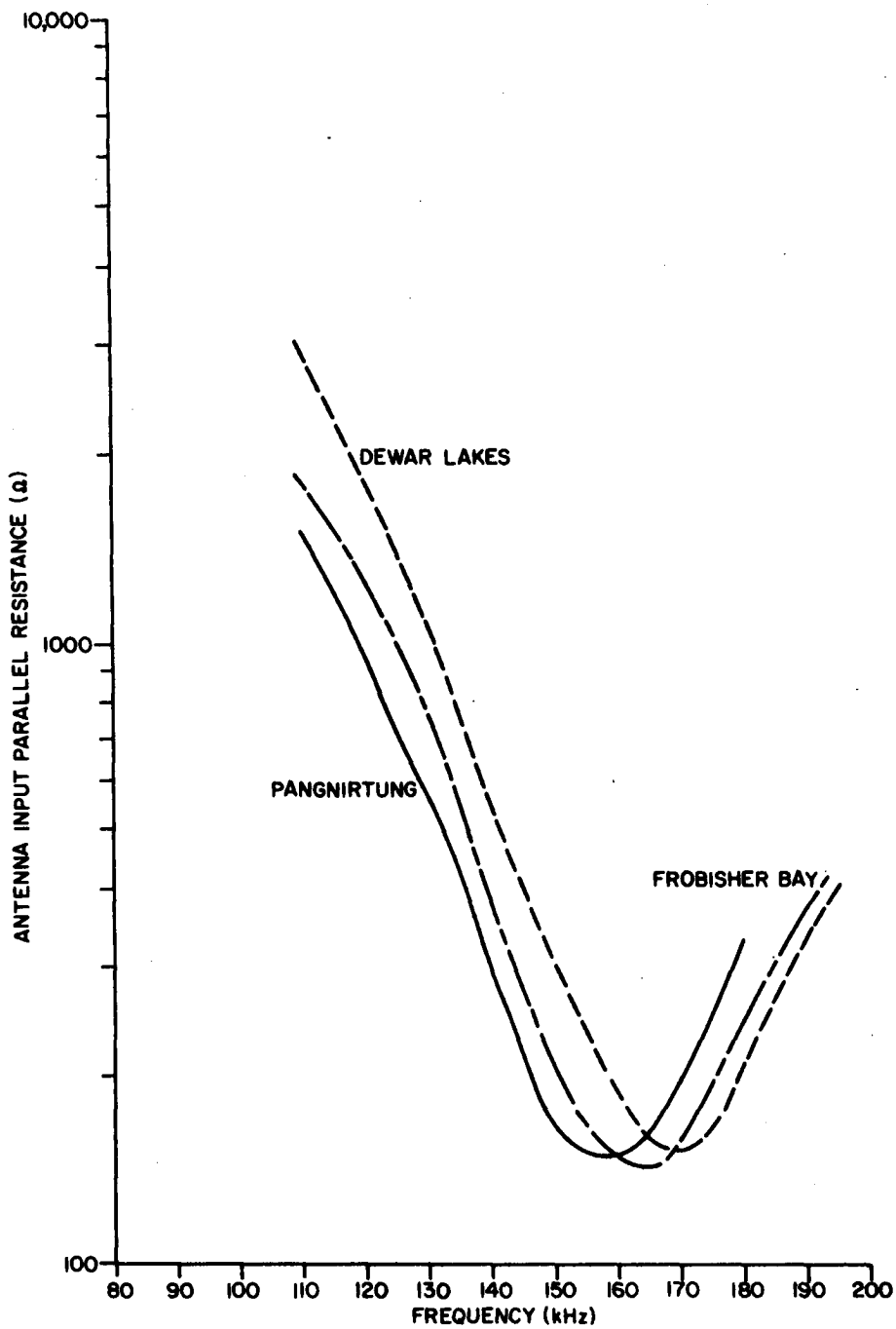

Fig. 11. Antenna input parallel resistances measured on Baffin Island

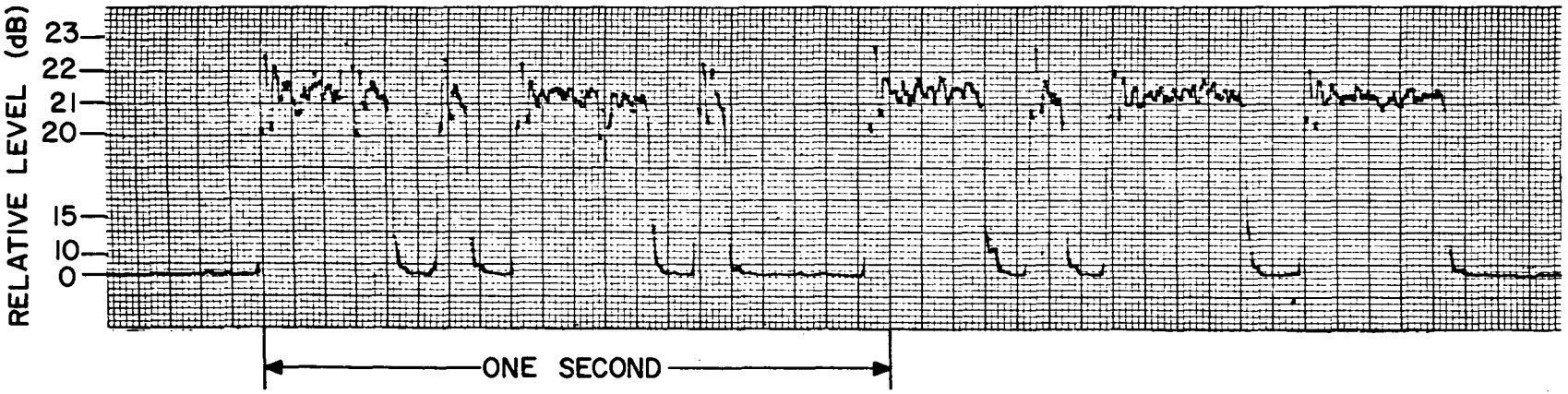

(A) 1630 HRS.

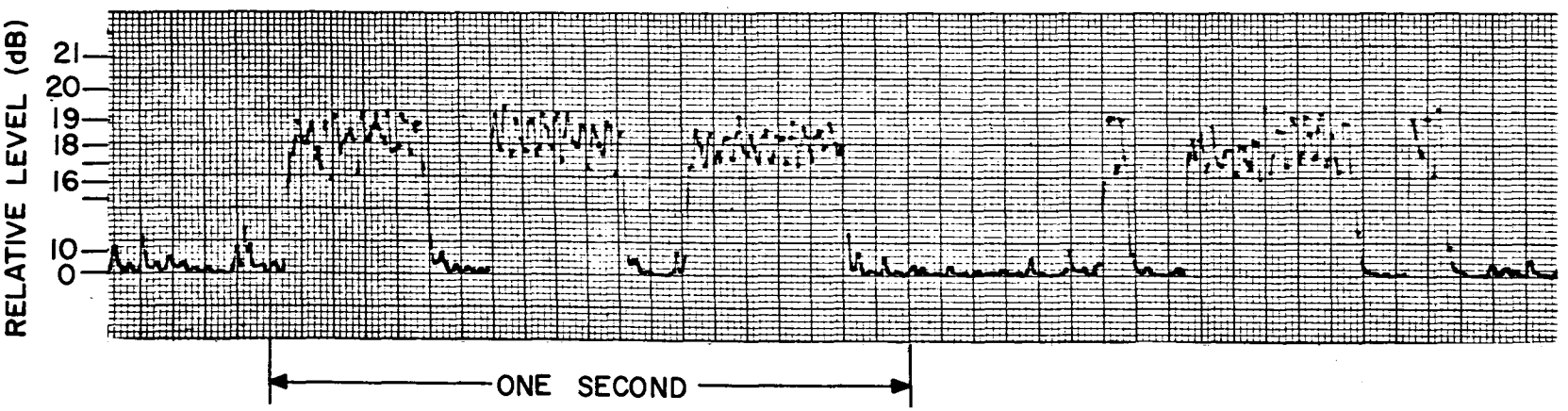

(B) 2230 HRS.

Fig. 12. Frobisher Bay - Pangnirtung (188 miles) signals, August 1969.

sea path between Frobisher Bay and Pangnirtung. With an input power of 300 watts, an antenna efficiency of -30 dB, a ground conductivity of 5×10^{-4} mhos/meter, and a noise level of one microvolt/meter, it can be shown that a 10 dB signal-to-noise ratio would have been achieved at a distance of 150 miles. This very likely represents the maximum range that could have been achieved under the circumstances existing in August. In the winter, the atmospheric noise would go down, and the range could be extended out to a maximum of 350 miles.

5.7 INUVIK TRIALS

In October 1969 the system was taken to Inuvik, N.W.T. for operational use during a Canadian Airborne Regiment exercise. However, inclement weather prevented the establishment of a second base and thus there was no opportunity to attempt communications.

It was possible, however, to conduct field intensity measurements over an 80 mile path between Inuvik and Tuktoyaktuk. The path is indicated on Figure 6. The terminal was deployed at Inuvik alongside a gravel road on a mixture of brush and mud. The permafrost started at a depth of about 3 feet.

The antenna input parallel resistance followed the characteristic shape shown in Figure B-4 of Appendix B and had a minimum value of about 150 ohms and a resonant frequency of approximately 200 kHz. This is one of the highest resonant frequencies measured during the entire program.

The antenna efficiency was measured to be -26 dB. Figure 13 shows the field intensity curve measured when the power input to the antenna was 330 watts. The slope of the curve suggests that the path conductivity was about 5×10^{-4} mhos/meter. Extrapolation of this curve indicates that a communications distance in excess of 400 miles would have been achievable at the time.

6. CONCLUSIONS

6.1 PRESENT SYSTEM

The experimental results of the field trials and demonstrations of the low frequency communications system indicate that such a system is capable of providing reliable communications over short distances in the Arctic. The system has been used at a wide variety of locations and during most seasons. It has always been able to provide Morse-code communications at a range of 200 miles.

There is no doubt that the system is small and light enough to be stowed away in an oversnow vehicle, ready for use in an emergency. Deployment is fast and easy, when done by vehicle, requiring very little human exposure outside the warmth of the vehicle. Therefore, it is felt that a system of this type (if production models were inexpensive enough) could fulfill the increasingly important requirement for emergency back-up communications in the Arctic at ranges up to 200 miles.

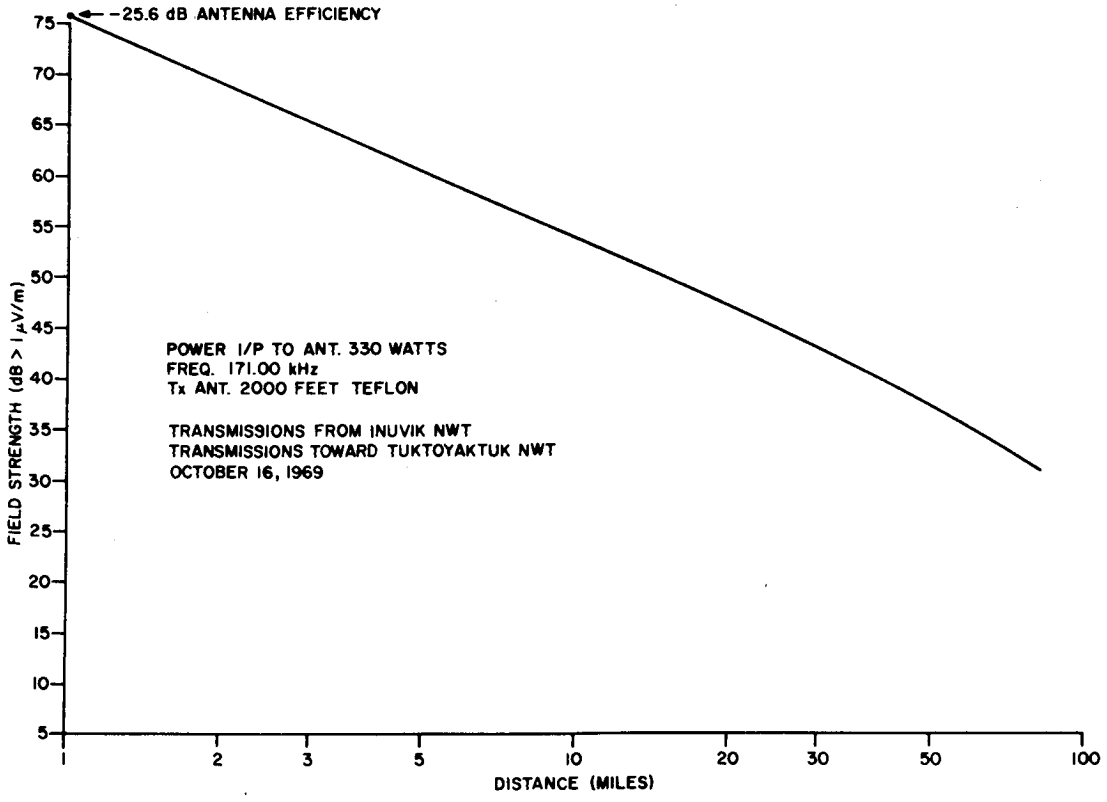

Fig. 13. Field strength attenuation curve measured between Inuvik and Tuktoyaktuk.

6.2 FURTHER WORK REQUIRED

A very extensive experimental programme would be required to establish accurately the range limitations of this system. Undoubtedly there will exist at some time and at some place, the necessary conditions that would limit this range to less than 200 miles. However, the expense of such a programme is probably not warranted since it is expected that such a system would be used mostly in the winter season when emergencies are more likely to occur, and it is during this season that the system should perform best.

Work at CRC on a new version of the transmitter has almost been completed. The new design employs only two transistors in the power amplifier instead of the six employed in the transmitter described in this report. This has increased the overall efficiency of the electronics. The heat sink design has been altered to allow the 100 per cent duty cycle operation required by FSK. This new design will be described in another CRC report when the work is completed.

7. REFERENCES

1. Watt, A.D. Coon, R.M., Maxwell, E.L., and R.W. Plush. *Performance of some Radio Systems in the Presence of Thermal and Atmospheric Noise.* Proc. IRE, Dec. 1958, pp 1914-1923.

2. International Telecommunications Union. *World Distribution and Characteristics of Atmospheric Radio Noise.* CCIR Report No. 322, Geneva 1954.

3. Norton, K.A. *The Calculation of Ground-wave Field Intensity Over a Finitely Conducting Spherical Earth.* Proc. IRE Dec. 1941, p. 623.

4. Maxwell, E.L. and R.R. Morgan. *A 10 kHz Effective Conductivity Map of North America.* AGARD/NATO Symposium on Sub-Surface Communications, April 1966, 25-29.

5. Seeley, E.W. and P.H. Wiborg. *Horizontal VLF Transmitting Antennas Near the Earth.* Naval Ordinance Laboratory, Corona Report 721, 15 May, 1967.

6. Weeks, W.L. and R.C. Fenwick. *Submerged Antenna Performance.* IRE International Convention Record 1962, Vol. 10, Pt. 1, page 108.

7. Chudobiak, W.J. and D.F. Page. *Frequency and Power Limitations of Class D Transistor Amplifiers.* IEEE J. of Solid State Physics, Vol. SC-4, No. 1, Feb. 1969, pp. 25-37.

8. Hindson, W.D. *A Portable 100 Watt LF Transmitter.* DRTE Technical Memorandum No. 501, May 1967.

9. Clevite Corporation Piezoelectric Division. *Ceramic Transfilters in Oscillator Circuits.* Bulletin 94-37.

10. Wait, J.R. *The Electromagnetic Fields of a Horizontal Dipole in the Presence of a Conducting Half-space.* Canadian J. of Physics, Vol. 39, 1961, pp 1017-1088.

11. Scherer, W.M. *Receiver Signal Handling Capabilities.* CQ, February 1970, pp 51-55.

12. Rheinfelder, W.A. *Designing Low-noise RF Input Transistor Stages.* Motorola Semiconductor Products, Application Notes.

13. Belrose, J.S. *The Use of a Screened Loop Antenna for Reception of Low Frequency Radio Waves.* DRTE, RPL Report No. 10-0-1, June 1962.

14. Watt, A.D. *VLF Radio Engineering.* Permagon Press, 1967, pp 415-436.

8. ACKNOWLEDGEMENTS

The author is indebted to many people of the Communications Research Centre for their advice, and in particular to W.D. Hindson and W.J. Chudobiak for their technical assistance in designing the transceivers. W.F. Haskell

and W.A. Hart constructed and tested the transceivers and participated in many of the demonstrations in the Arctic.

The author would like to extend his thanks to Major Batt and his able group of signallers from the Canadian Airborne Regiment who participated in the field demonstrations at Watson Lake, Frobisher Bay and Inuvik.

The work was initiated at the Defence Research Telecommunications Establishment of the Defence Research Board and continued under the sponsorship of DRB when DRTE was transferred to the Department of Communications in April 1969 and named the Communications Research Centre.

APPENDIX A

ATMOSPHERIC NOISE LEVEL PREDICTIONS

1. INTRODUCTION

The CCIR has summarized existing data on atmospheric noise in its Report 322[2] in an attempt to aid the communications system designer in the determination of the minimum signal level required for satisfactory system performance. The data have been grouped together for each of the four seasons and for each of six, four-hour periods of the day. The aggregate of corresponding four-hour periods of the day throughout a season is defined as a time block. Report 322 presents the median hourly value of the average noise power for each time block and for all geographical locations, and variations within a time block are treated in a statistical manner. The mean noise power forms the basis of the CCIR report.

The noise power received from sources external to the antenna is expressed by an effective antenna noise factor, F_a, which is related to the rms noise field strength, E_n by the following formula:

$$E_n = F_a - 99.5 + 20 \log_{10} f + \log_{10} b$$

where f is the frequency in MHz,

F_a is in dB

E_n is in dB>1μV/m

and b is the receiver bandwidth in Hz.

The median hourly value of F_a within a time-block is designated as F_{am}. The value of F_a exceeded 10 per cent and 90 per cent of the time within a time-block, are expressed as deviations D_u and D_ℓ from F_{am}.

The short-term characteristics of the noise are described by the amplitude-probability distribution curves for the noise envelope.

In the CCIR Report, these distribution curves are drawn so that a Rayleigh distribution (representing the envelope of thermal noise) is a straight line with a slope of $-\frac{1}{2}$. It is interesting to note that the low levels of the atmospheric noise distributions are Rayleigh in shape, but that the higher levels have a greater slope. It has been found that the ratio of rms noise voltage to average noise voltage, F_d, is sufficient to specify the distribution

curve. Estimates have also been made of the uncertainties in the distribution curves. These are expressed as the probability of a standard deviation σ_Δ of Δ, (the difference between the instantaneous envelope amplitude and the rms value of the noise). These uncertainties are all expressed in graphical form in the CCIR Report.

The CCIR Report also includes values of the standard deviation of F_{am}, σ_{Fam}, which have been derived by comparing actual observations with predictions.

2. NOISE LEVEL PREDICTIONS FOR CANADA'S NORTHERN COASTLINE

For these calculations the following assumptions are made:

(i) Season: for maximum noise - summer
for minimum noise - autumn

(ii) Time: for maximum noise - 2000-2400 hours
for minimum noise - 0800-1200 hours

(iii) Receiver Bandwidth: 100 Hz

(iv) Propagation: ground-wave (i.e., steady signal)

(v) Frequency: 100 and 200 kHz

(vi) Modulation: On-off Morse code keying

(vii) Grade of Service: noise envelope must not exceed carrier envelope for more than 0.1 per cent of the time.

The Figures mentioned in this section refer to the Figure numbers in reference (2).

Using the geographical location, season and time of year, the following parameters are determined from Figures 19 and 22.

PARAMETERS	Maximum Noise Frequency		Minimum Noise Frequency	
	100 kHz	200 kHz	100 kHz	200 kHz
Fam(dB>KTB)	102	85	90	65
σ_{Fam}	3.8	4.2	11	8.6
D_u	7.8	9	16.5	17
σ_{Du}	2.5	3	4	5
$F_o=F_{am}+D_u$	109.8	94	106.5	8.2
$\sigma_{Fa}=\sigma_{Fam}+\sigma_{Du}$	6.3	7.2	15	13.6
E_n(100 Hz BW) in dB>1μV/m	14.3	4.5	11.0	-7.5

APPENDIX B

PARAMETERS OF A DIPOLE ANTENNA LYING ON THE SURFACE OF THE EARTH

1. FAR ZONE FIELDS

Using equations developed by Wait[10] it follows that:

a) the vertical field component is maximum along the axis of the antenna;

b) the horizontal field component is attenuated very rapidly by the earth; and

c) the field strengths depend on the ratio of the propagation constant in free space to that in the ground $\frac{\delta_0}{\delta_1}$; δ_1 is naturally dependent upon the electrical characteristics of the ground, and as the conductivity decreases, δ_1 approaches δ_0 and the fields become stronger. In other words, the lower arctic ground conductivity will enhance the horizontal antenna's performance.

Figure B-1 compares the theoretical antenna pattern in the horizontal plane with the measured pattern, for a 2000 foot dipole.

2. IMPEDANCE

The theoretical analyses in the literature[5,6] normally treat the horizontal dipole lying on the earth as a lossy transmission line. The current distribution and input impedance to the antenna can then be calculated if the propagation constants have been determined. These constants depend greatly on the electrical parameters of the earth and the difficulty in arriving theoretically at suitable constants arises from the problem of adequately modelling the true earth.

Reference (6) has derived equations for the series input resistance and reactance for a submerged dipole. Figures B-2 and B-3 compare the theoretical resistance and reactance, as calculated from the equations using the earth parameters shown, with the actual measurements made on the antenna. As can be seen, the model very closely predicts the reactance but is inaccurate for input resistance. An attempt was made to vary the earth parameters to get closer agreement between the theoretical and measured curves, but not much success was achieved. This indicates that the actual conditions were not represented adequately by the model in reference (6).

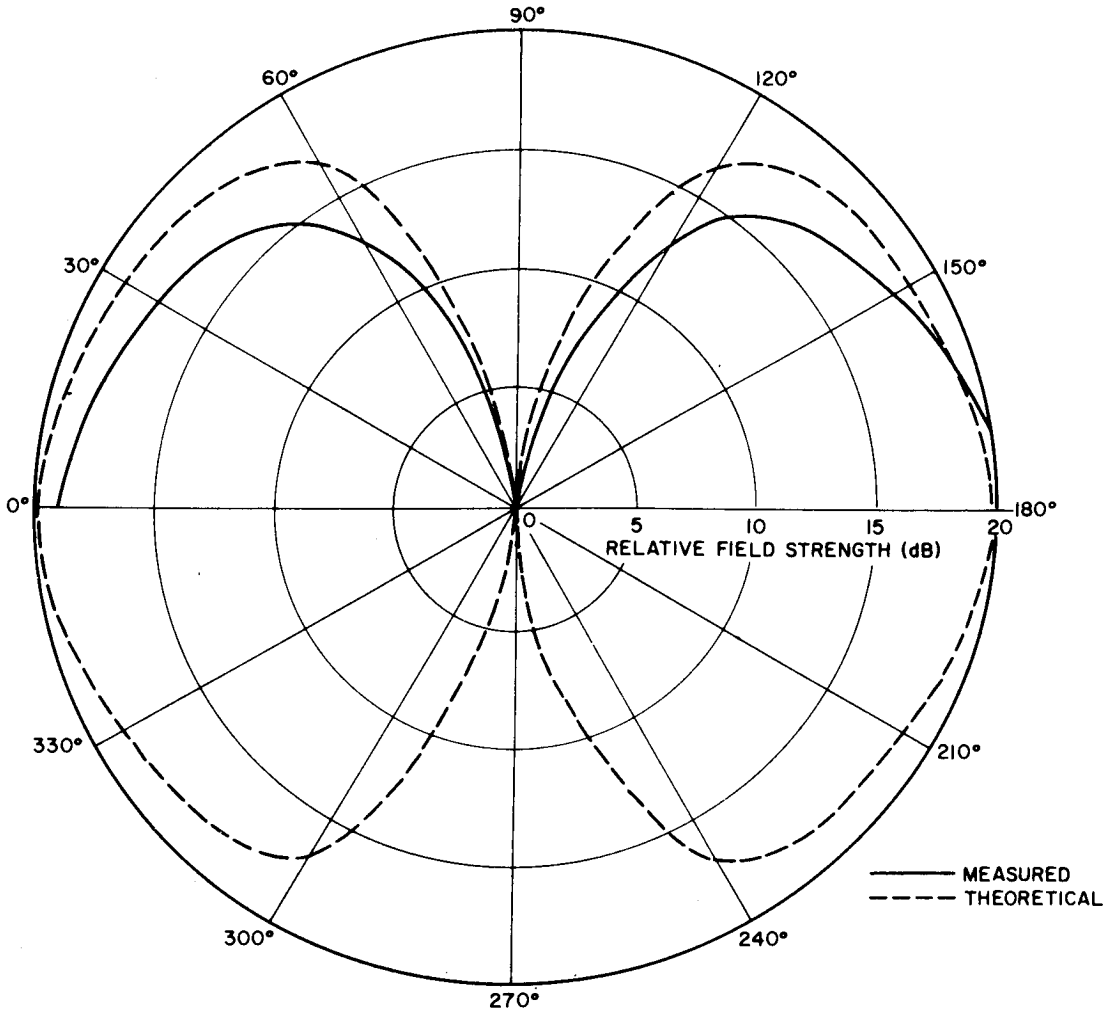

Fig. B-1. Azimuthal patterns for vertically polarized radiation from a dipole lying on the surface of the earth.

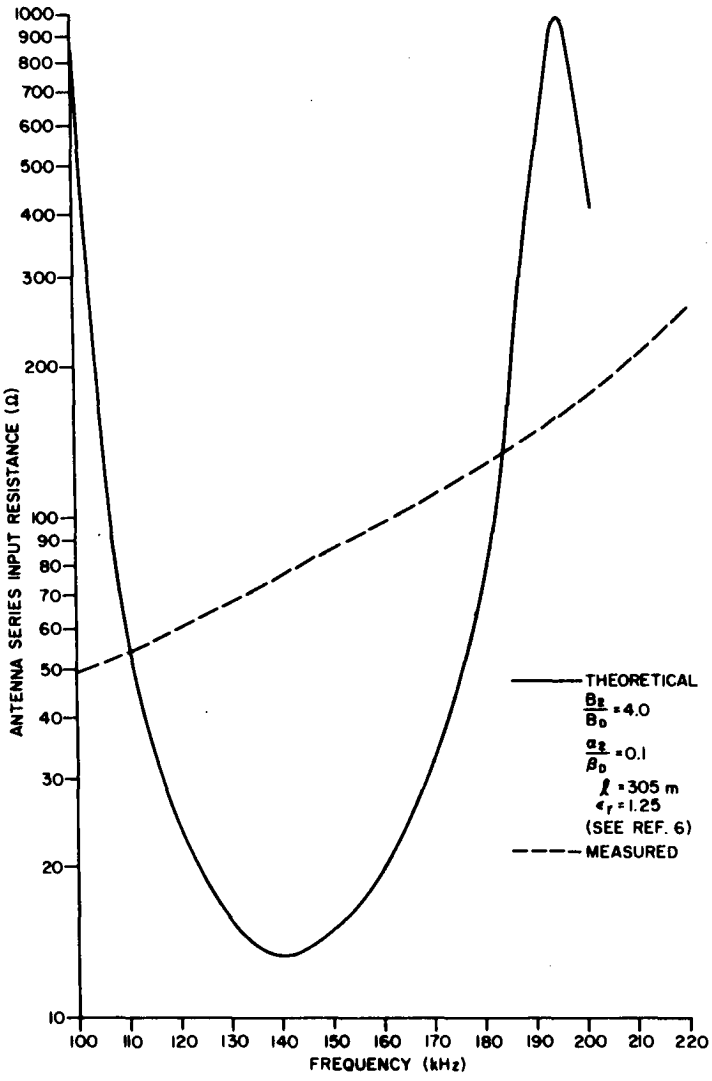

Fig. B-2. Antenna series input resistance for a 2000 foot dipole lying on the surface of the earth.

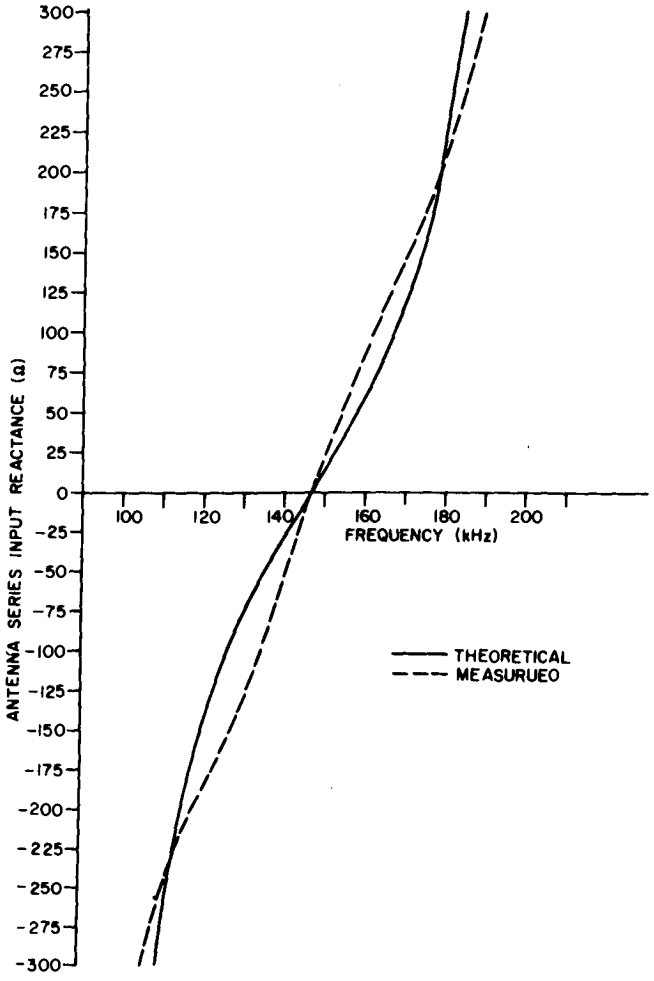

Fig. B-3. Antenna series input reactance for a 2000 foot dipole lying on the surface of the earth.

Because of the dependence of the input impedence on the earth parameters, it is expected that this impedance would change as the antenna is deployed over different terrains. Figure B-4 shows how the parallel input resistance varies with different antenna locations. The parallel values are used here because it is these values that are used directly in the tuning procedure for the transmitter. The large variation in input resistance with both frequency and earth condition dictates the necessity for a wide tuning range in the transmitter.

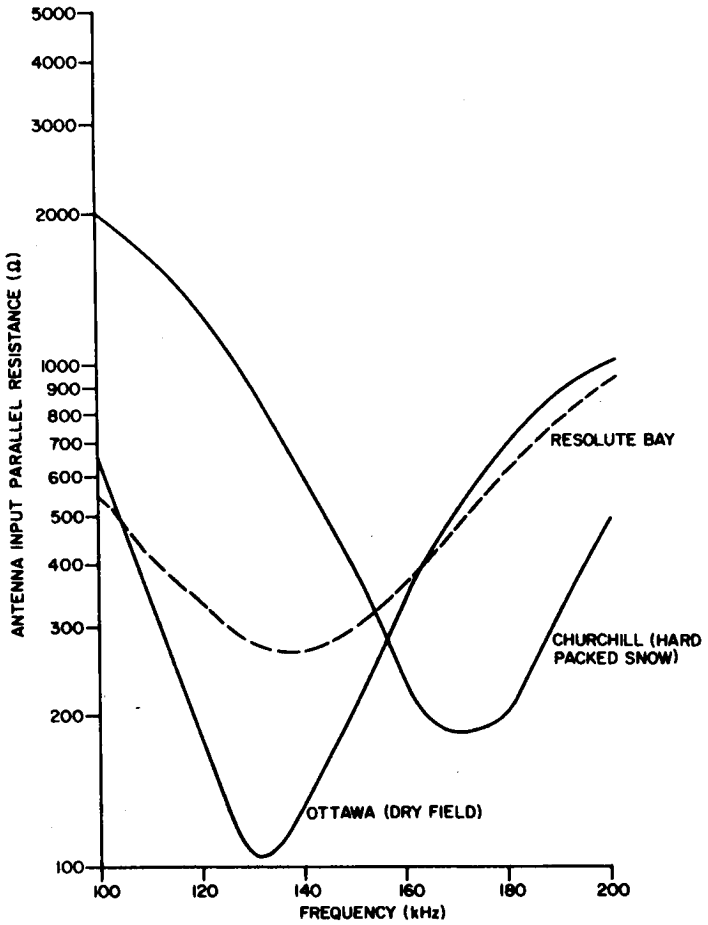

Fig. B-4. Antenna input parallel resistances for dipole lying on different types of ground.

3. ANTENNA CURRENT DISTRIBUTION

The theoretical current distribution is determined from the transmission line model mentioned above. For a 2000 foot dipole operating in the region from 100 to 200 kHz, the theoretical distribution is sinusoidal. The actual current distribution and the theoretical distribution are compared in Figure B-5.

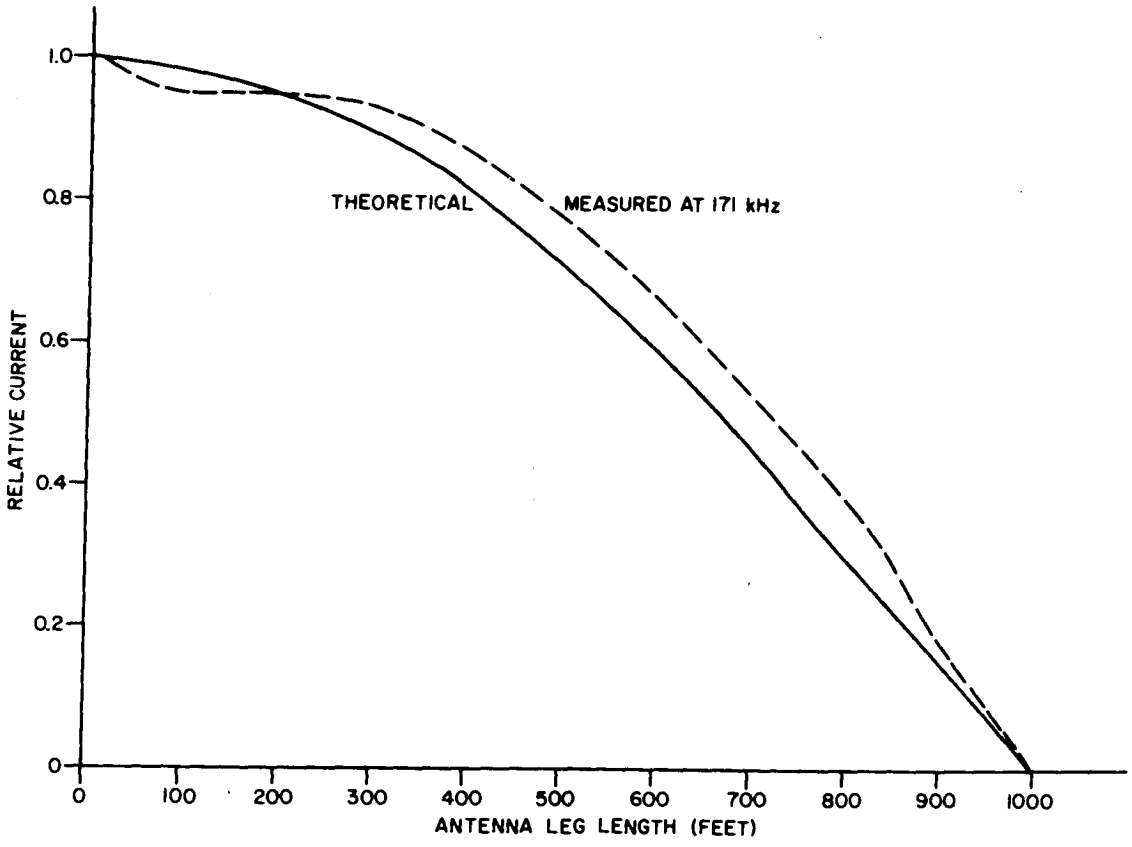

Fig. B-5. Antenna current distribution.

4. ANTENNA EFFICIENCY

With the dipole antenna in a lossy environment it is difficult to apply the conventional definitions of gain and efficiency. For the purposes of this paper, the following definition[6], is used to define antenna efficiency:

$$\text{Relative communications efficiency} = \frac{\text{Power density at receiving position when the test antenna is transmitting}}{\text{Power density at receiving position when a quarter-wave vertical monopole is transmitting.}}$$

This definition assumes equal input powers to both antennas. The theoretical efficiency can be calculated by using the following formula[6]:

$$\eta = \frac{144}{R_s} \left|\frac{1}{n}\right|^2 \left(\frac{F}{1 - F^2}\right)^2 \left(\cos \frac{F}{2}\right)^2$$

where

η = efficiency

R_s = input series resistance

n = the complex index of refraction of earth = $\sqrt{\varepsilon_r - j\frac{\sigma}{\omega\varepsilon_0}}$

$F = \frac{\text{measured resonant frequency}}{\text{resonant frequency in air}}$

σ = ground conductivity

ε_r = relative dielectric constant of the earth

ε_0 = dielectric constant of free space

ω = radian frequency of the transmission

For the conditions considered in this paper the following approximation can be made:

$$\left|\frac{1}{n}\right|^2 \simeq \frac{\omega\varepsilon_0}{\sigma} .$$

It can thus be seen that the antenna efficiency is inversely proportional to the ground conductivity and independent of the dielectric constant of the ground.

Accurate field strength vs distance measurements have been made in the Ottawa area using a 2000 foot dipole and these show that the ground conductivity is approximately 5×10^{-4} mhos/meter. The measured antenna efficiency for this case was -20.4 dB at a frequency of 200 kHz. The measured parameters needed for the theoretical calculation of efficiency are: R_s = 154 Ω and F = 0.61. The calculated theoretical efficiency thus becomes -21.9 dB.

The same antenna described above has had its efficiency reduced by more than 10 dB when measurements were taken after a heavy rain storm. This loss of efficiency would have serious effects on the communications range of the system and it is for this reason that any system designs should be based on a worst case efficiency of -30 dB.

APPENDIX C

LOW FREQUENCY SOLID STATE TRANSMITTER

1. INTRODUCTION

The recent advances in solid-state devices have permitted the application of class D amplifiers to relatively high powered low frequency transmitters. This allows the efficient transfer of dc power to RF power and permits the design of an all solid-state 400 watt ttansmitter. A comprehensive understanding of class D amplifiers can be obtained from reference (7) and only a summary of the amplifier characteristics will be given here.

Class D amplifiers can be defined as "amplifiers where the active devices have a conduction angle of 180° and conduct appreciable currents only while in the saturated state". Figure C-1 shows the basic circuit for the current switching class D amplifier and various voltage and current waveforms. The circuit is essentially a dc-ac converter where the input signal switches the two transistors between cut-off and saturation with a phase difference of 180° between Q1 and Q2. This results in the constant current, supplied by the inductor L2, being alternately switched between the two transistors, thereby producing antiphase square wave pulses of collector current. The voltage at each collector is a half-sinusoid because of the action of the tuned tank circuit.

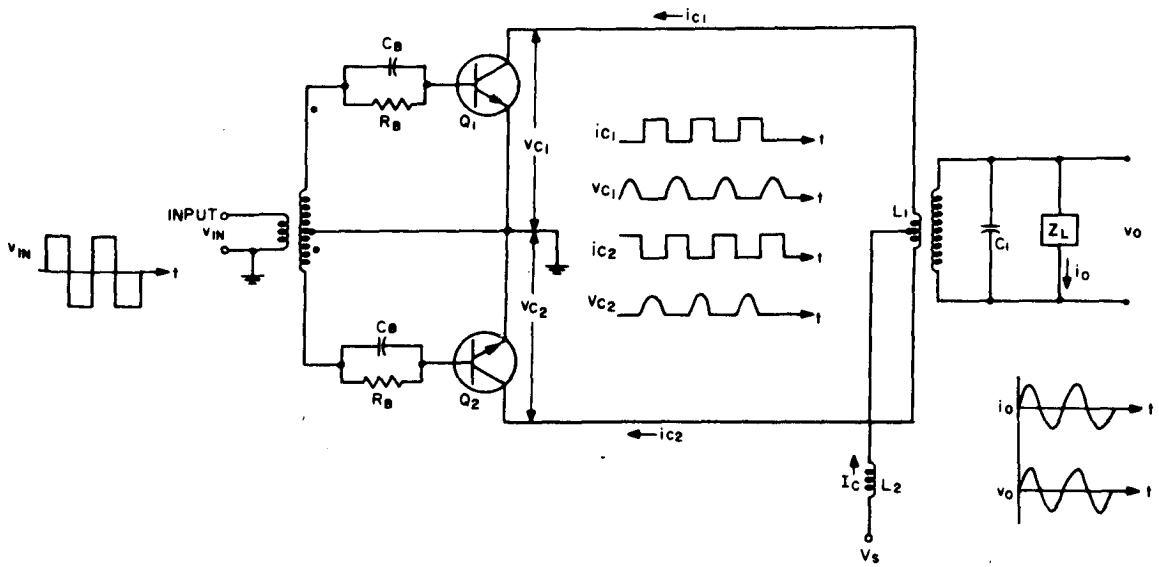

Fig. C-1. Current switching class D amplifier.

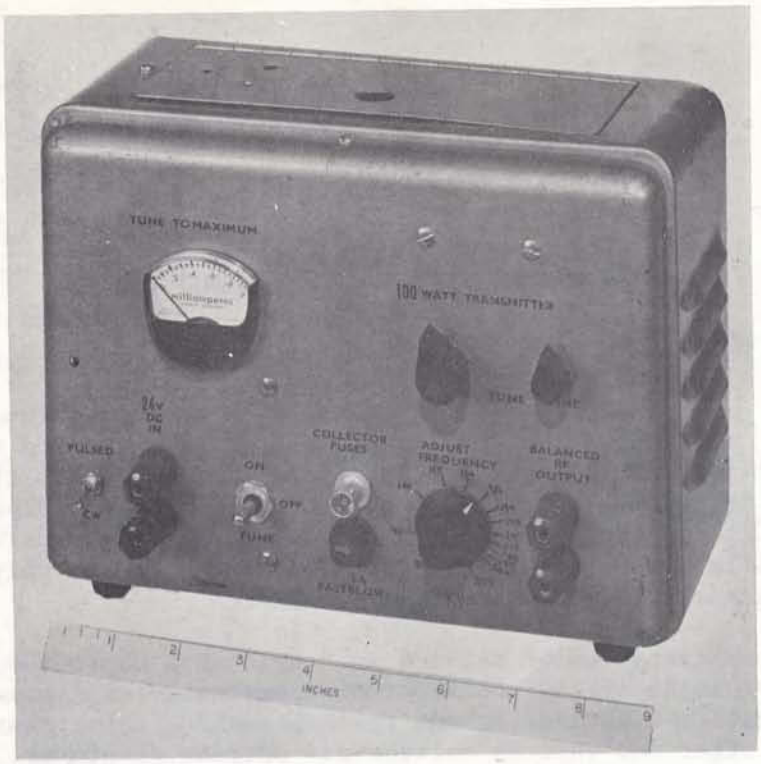

Fig. C-2. LF Transmitter MKI (100 watts).

Fig. C-3. LF Transmitter MKII (500 watts).

As can be seen from the ideal waveforms shown, the transistors have a 180° conduction angle, and only draw appreciable currents when saturated. Since the power dissipated in each transistor is the product of v_c and i_c, the waveforms show clearly that very little power is dissipated in the transistors. This is the key to the very high efficiencies obtainable from such an amplifier. In practice, the collector-emitter voltage of the transistor during saturation (V_{SAT}) is not zero and thus during the conduction half-cycle the power dissipated in the transistor is the product of V_{SAT} and I_c. Power is also dissipated during the switching times from cut-off to saturation and vice versa. Therefore, it is necessary to decrease the switching times to reduce this latter source of inefficiency and for this reason the input waveform is shown as a square wave and C_B has been added to each base circuit.

R_B defines the "ON" base current and therefore affects the value of V_{SAT} as well as the turn-off time of the transistors. A base drive current that is insufficient for a given I_c will not saturate the transistors and high dissipation will result. On the other hand, too much base drive will result in the device capacitive storage phenomenon degrading efficiency.

The tuned tank circuit recovers the fundamental frequency from the square wave.

The application of this circuit to high powered transmitters has required transistors with high current capacity and high voltage breakdown characteristics. The introduction of epitaxial silicon power transistors has made such circuits practical.

2. TRANSMITTER DEVELOPMENT

The author is indebted to Mr. W.D. Hindson, who, while attached to the Electronics Laboratory of the Defence Research Telecommunications Establishment, designed and constructed two complete low frequency transmitters for this project. The first transmitter was a 100 watt device capable of operation from 100 to 200 kHz and is described in reference (8). Figure C-2 is a photograph of this device. The second transmitter was capable of 500 watts of RF output and included more sophisticated protection circuitry, variable output impedance matching networks and monitoring devices. This unit is shown in Figure C-3. The design of the final transmitter, built as part of a transceiver for system evaluation, was based on Mr. Hindson's work and is described in detail in the next section.

3. LOW FREQUENCY TRANSMITTER CIRCUIT DESCRIPTION

3.1 Signal Source

Figure C-4 is the signal source circuit diagram, and Figure C-5 shows typical waveforms obtained at the points indicated. The oscillator is a modified Clapp-circuit with crystal control and collector-to-base regeneration. This type of circuit is particularly useful when the frequency range to be

covered is as wide as it is here (100 - 200 kHz), since frequency selection involves only the choice of the proper crystal. The 390 μH and 56 μH coils are added in series with the crystals to make the oscillator output frequencies coincide exactly with those desired. The system design allows for a ±5 Hz variation from the desired center frequency over the temperature range from -40° to +50°C and over a voltage range from +18 to +28 volts. The crystals are located in a 75°C oven and were chosen to provide an oscillator frequency twice the desired frequency. The frequency is halved again at the output amplifier. This allows the use of the smaller sized crystals in the standard HC-6/U holder.

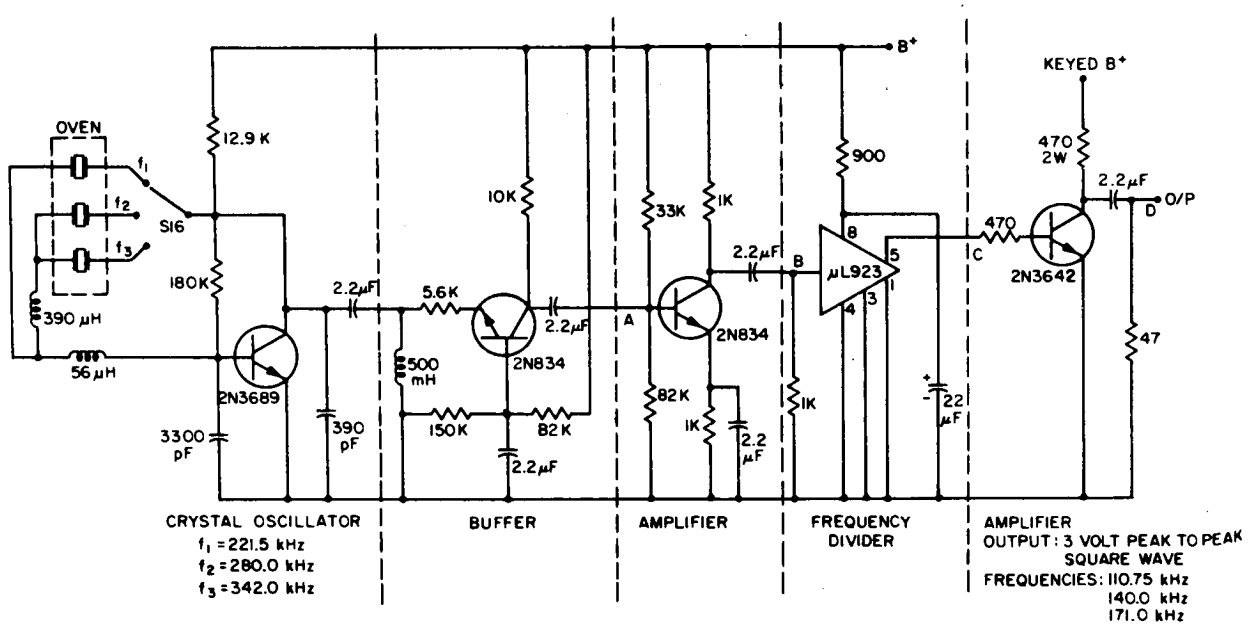

Fig. C-4. Transmitter signal source circuitry.

The second stage of the signal source circuitry is a common base amplifier used as a buffer. This type of amplifier has a low input impedance and with the base at ac ground the oscillator sees a constant load, which in this case is 5.6 kΩ. The waveform of figure C-5(a) shows the output of the buffer.

The buffer is followed by one stage of amplification before the signal is applied to the μL923 integrated circuit. Figure C-5(b) shows the waveform at the output of the first amplifier. The μL923 is used as a saturating frequency divider and produces a square wave output at exactly half the frequency of the input. Figure C-5(c) shows the waveform at the output of the μL923.

The second amplifier produces an output of at least 2 volts peak to peak across a 47Ω load. The voltage at this point is shown in Figure C-5(d). It is this voltage which is applied to the final drive circuitry. The B+ supply to

this final amplifier is keyed by the modulation circuit so that the oscillator output is only applied to the final drive circuitry when the transmitter is keyed on.

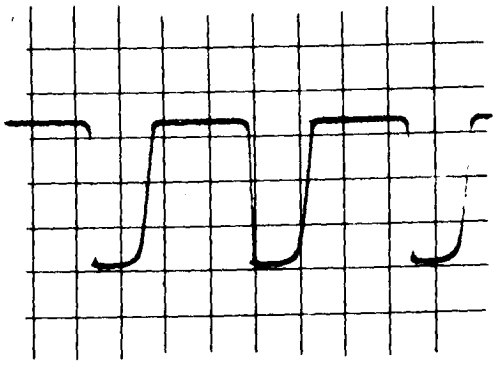

(A) BUFFER O/P
0.5V/cm
f = 280kHz

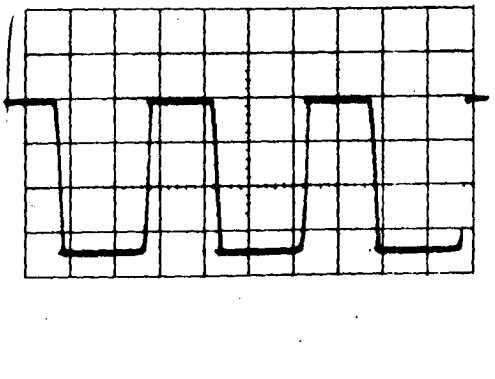

(B) FIRST AMPLIFIER O/P
2.0V/DIV.
f = 280kHz

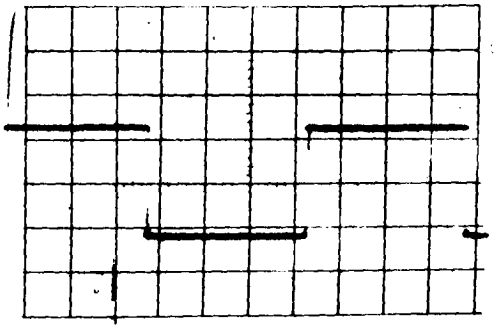

(C) FREQUENCY DIVIDER O/P
0.5V/DIV.
f = 140kHz

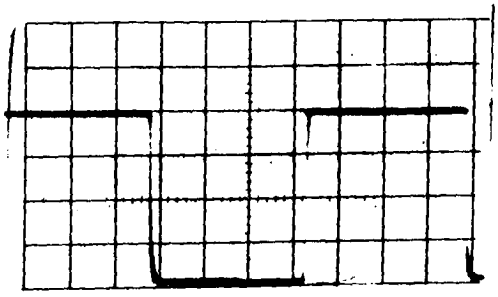

(D) SECOND AMPLIFIER O/P
1.0V/DIV.
f = 140kHz

Fig. C-5. Transmitter signal source waveforms.

3.2 Final Drive

The signal input to this stage is normally derived from the transmitter signal source, but it is also possible to use an external signal. In either case at least 10 MW of signal power is required.

Figure C-6 is the circuit diagram for the final drive. The two 1N4151 diodes across the input limit the maximum signal to the circuit. This signal is transformer coupled to the pair of 2N834 transistors which operate as a

saturating differential amplifier. The output of this circuit is a square-wave. Although the internal signal source is already a square wave, this circuit is included to allow an external sine wave oscillator to drive the transmitter. (A strictly operational unit would only have an internal signal source and consequently, this first stage of the circuitry could be eliminated.) Figure C-7(a) shows the voltage waveform at the primary of T_2 when a 1 volt rms sine wave signal is applied to the input. Point A on Figure C-6 shows the measuring point.

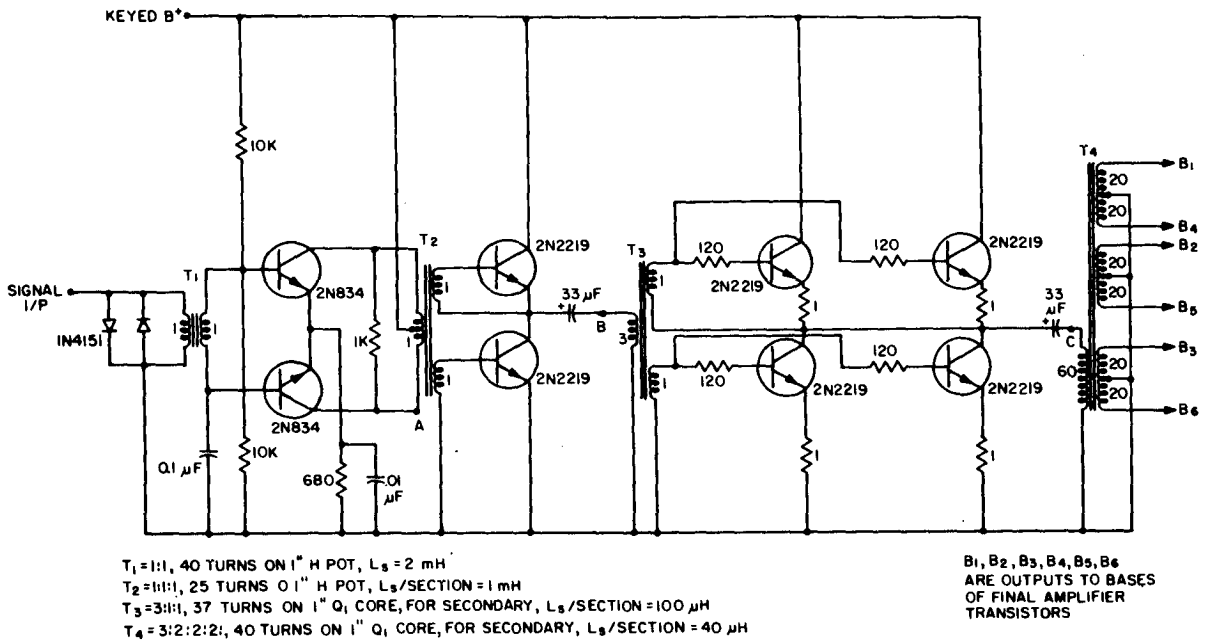

Fig. C-6. Transmitter final drive circuitry.

The next stage is a pair of 2N2219 transistors operating as Class D saturating current amplifiers. Figure C-7(b) shows the voltage waveform at the primary of T_3 (point B in Figure C-6).

The final stage is a parallel pair of 2N2219 transistors operating as a Class D saturating current amplifier. The output of this stage is transformer coupled to the base of each power amplifier transistor and supplies about 300 mA of base current to each. Figure C-7(c) shows the voltage waveform at the primary of T_4 (point C in Figure C-6). Figure C-7(d) shows the same waveform but with an expanded time scale. From this it can be seen that the rise time for the square wave pulse is about 1.1 μsec.

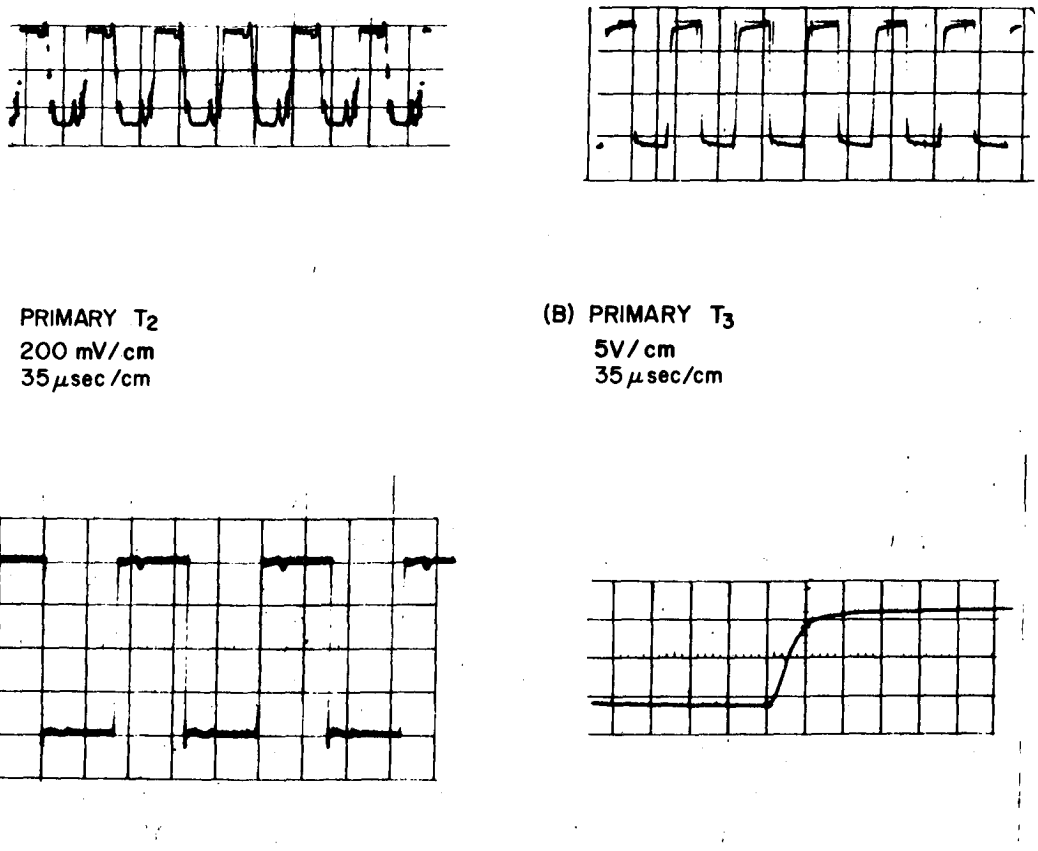

Figure C-7. Transmitter final drive waveforms.

The B+ supply to the entire circuit is keyed by the modulator circuit so that drive is only supplied to the power amplifier when the transmitter is keyed on.

3.3 Power Amplifier

Figure C-8 is the circuit diagram of the power amplifier, and as can be seen, it is basically the same circuit as Figure C-1. Instead of having just one transistor per side, there are now three transistors in parallel on each side. This has been done to increase the power output of the transmitter. The 0.006Ω resistors in each emitter have been added to force the transistors to share the current equally. The individual base driver circuits labelled B_1 to B_6 correspond to the output transformer labelling in Figure C-6.

The leakage inductance of T_5 is an important factor, causing high voltage spikes when the constant current is switched from one side of the amplifier to the other. Increasing the leakage inductance increases the amplitude of the voltage spikes. The TA2669A transistors have a maximum collector-to-emitter sustaining voltage of 110 volts with an external base-to-emitter

resistance less than 50Ω. Thus, to protect the transistors from the leakage inductance voltage spikes, 1N3339A 50 watt 91 volt zener diodes are connected from each collector to ground.

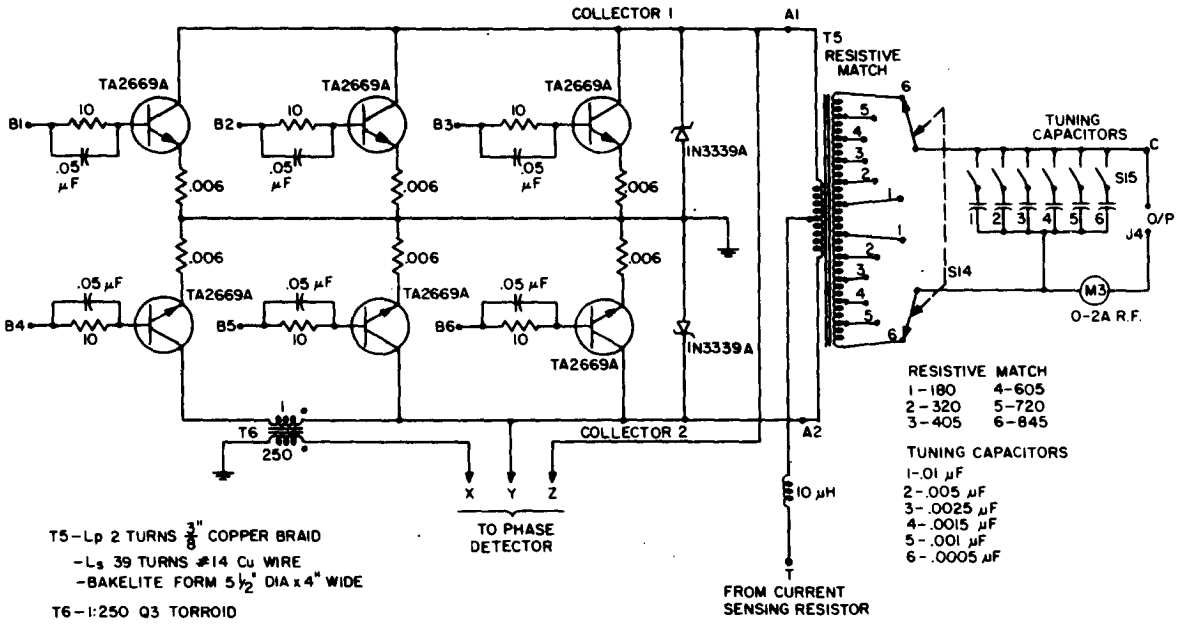

Fig. C-8. Transmitter power amplifier circuitry.

T_5 is a step up transformer which matches the desired collector impedance to the load impedance. The load impedance can vary from 100 to 1000Ω. The tank circuit and load reactances are tuned out with a bank of tuning capacitors.

Figure C-9(a) is a comparison of the two collector voltage waveforms. These correspond to the two ideal waveforms v_{c_1} and v_{c_2} of Figure C-1 and are 180° out of phase. The voltage spike caused by the leakage inductance of T_5 is clearly visible and is occasionally limited by the zener diodes.

Figure C-9(b) compares the voltage at collector 1 with the current flowing in the collector 1 circuit. These correspond to the waveforms of v_{c_1} and i_{c_1} of Figure C-1 and are 180° out of phase.

Figure C-9(c) shows the output voltage developed across a 720Ω resistive load.

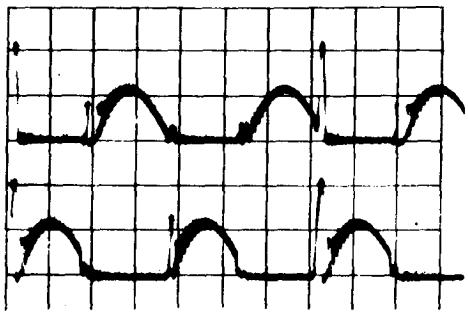

(A) UPPER - COLLECTOR 1 VOLTAGE
LOWER - COLLECTOR 2 VOLTAGE
50V/cm 2μsec/cm

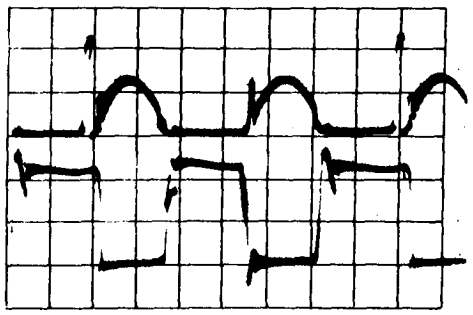

(B) UPPER - COLLECTOR 1 VOLTAGE - 50V/cm
LOWER - COLLECTOR 1 CURRENT - 10A/cm
2μsec/cm

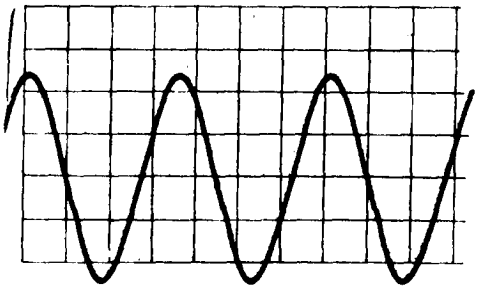

(C) OUTPUT VOLTAGE ACROSS 720Ω
RESISTIVE LOAD. 350 WATTS AT 140kHz.

Fig. C-9. Transmitter power amplifier waveforms.

3.4 Phase Detector Circuitry

The transmitter is tuned to resonance by observing the output of the phase detector circuit. Figure C-8 shows that T_6 supplies a signal to the phase detector circuit (see Figure C-10) that is in phase with the collector current flowing in one side of the power amplifier. The signal from T_6 is a series of square wave current pulses and is applied to the phase detector circuit at point X. The pulses are amplified and applied to the emitters of the differential pair at points Y and Z. At resonance in the power amplifier the current pulses at X and the voltage at Z are in phase. This results in the square-wave current flowing through the right-hand differential transistor. When resonance is not attained the current will split between the two transistors. The potential difference across the meter is obviously a maximum at resonance and thus the tuning procedure simply requires maximizing the tuning meter deflection.

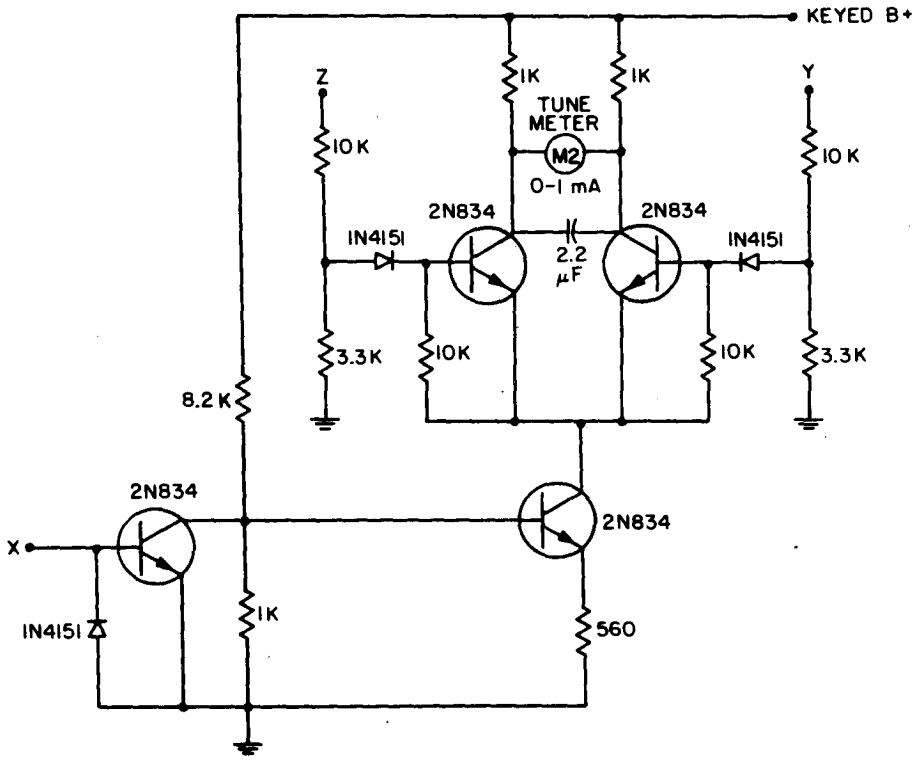

Fig. C-10. Transmitter phase detector circuitry.

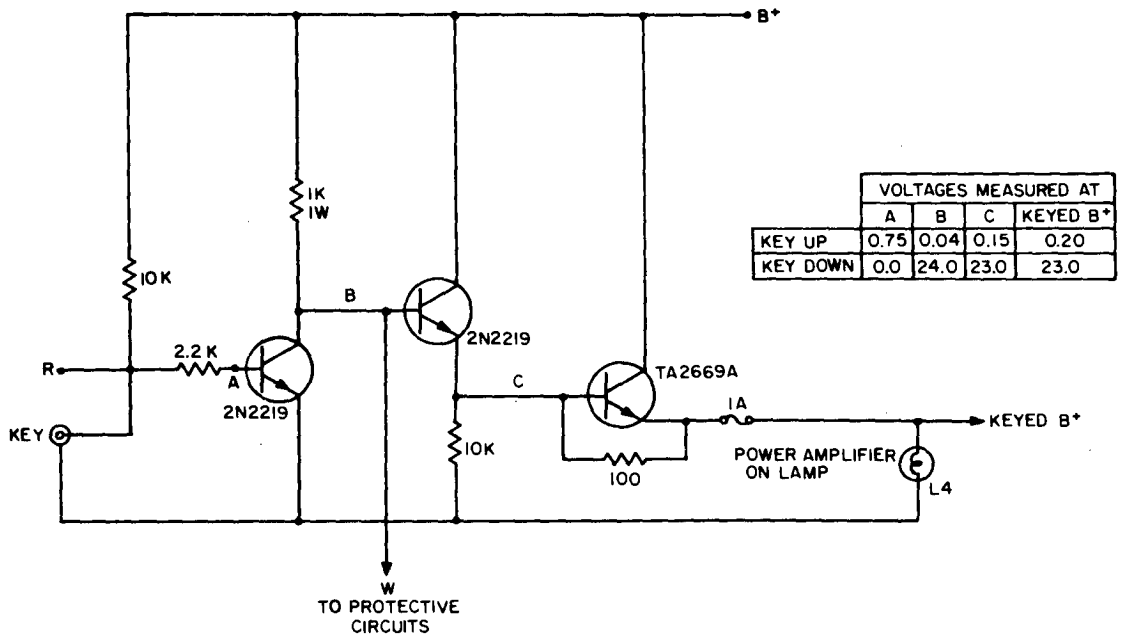

	VOLTAGES MEASURED AT			
	A	B	C	KEYED B+
KEY UP	0.75	0.04	0.15	0.20
KEY DOWN	0.0	24.0	23.0	23.0

Fig. C-11. Transmitter modulator circuitry.

3.5 Modulator Circuit

One of the basic differences between this transmitter and the previous models is the method of keying. The previous keying technique involved switching the B+ to the power amplifier. Circuits were required that could interrupt 30 amperes at the Morse code rate. Such circuits were developed, but device failure was a common occurrence resulting in the transmitter being turned on continuously. The technique used in this transmitter switches the drive to the final amplifier, a low power level circuit, and simplifies the design of a reliable modulation circuit.

Figure C-11 shows the modulator circuit and the various base and collector voltages for the "OFF" (key up) and "ON" (key down) conditions. The keyed B+ output is applied to the final amplifier of the signal source circuitry, to the final drive, and to the power amplifier "ON" lamp. To turn the transmitter on requires the grounding of point "R". The circuit diagram shows the Morse code key, but any circuit that grounds point "R" will turn the unit on.

Point "W" is connected to the protective circuits which ground this point when activated. When point "W" is grounded by the protective circuits, the transmitter is turned off and cannot be turned on until the reset button is activated, thereby lifting the ground from point "W".

3.6 Protective Circuits

In a unit intended for demonstrations and field use, it is necessary to provide sufficient protection for the active devices so that all transients and possible load irregularities will not cause permanent damage to the unit. The circuits employed in this transceiver monitor the following three parameters: (1) supply polarity (2) input current and (3) power amplifier zener diode temperature. Figure C-12 shows all the protective circuitry.

The reverse polarity circuit is simply a diode, a fuse and a 1/4Ω resistor. With proper supply polarity, the diode is reverse biased and draws negligible current. However, when the polarity is reversed the diode is forward biased and a large current starts to flow through the 1/4Ω resistor. This current is sufficient to blow the 30A fuse.

The current sensing circuit actually measures the voltage drop across the .002Ω resistor inserted in the supply line to the power amplifier. When the voltage across the resistor reaches a predetermined level (corresponding to, say, 30A current) the inputs to the integrated operational amplifier, LM107, reverse polarity and the output voltage on pin 6 rises sharply. This voltage is applied to the gates of the two silicon controlled rectifiers (SCR's) and the transmitter is turned off.

The current sensing circuit has been carefully designed to ensure that the operating point does not vary appreciably with supply voltage variations or temperature. The two 10K potentiometers are made from low temperature coefficient wire and therefore maintain the same voltage divider ratio regardless of temperature. This ensures that the voltages applied to the inputs are not temperature sensitive. The zener diode 1N3024A ensures that there is a constant voltage across the reference potentiometer but allows the absolute

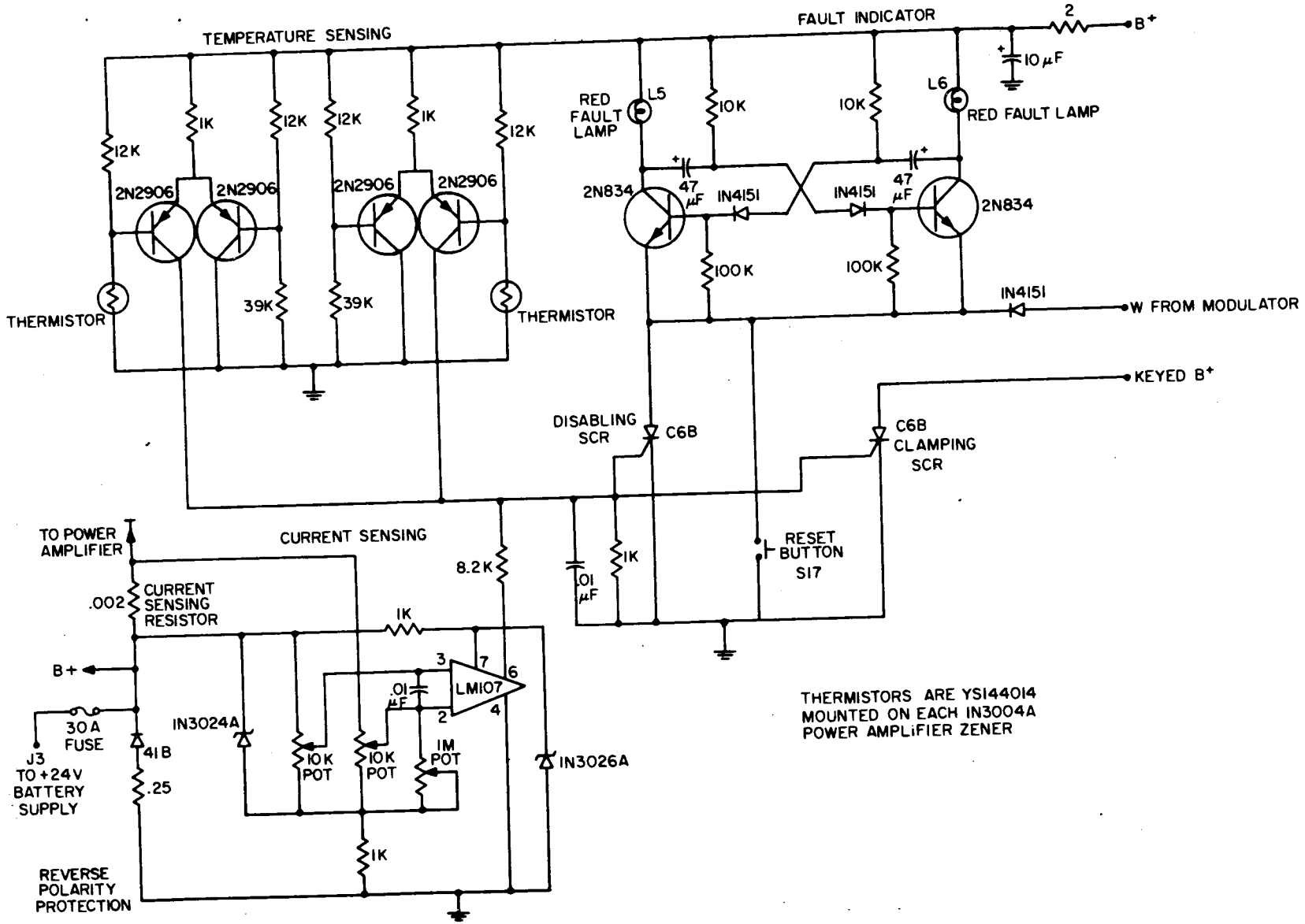

Fig. C-12. Transmitter protective circuitry.

reference voltage applied to input pin 3 to float with the changes in supply voltage. Finally, the 1N3026A zener makes the operational amplifier independent of supply voltages in the range 18-28 volts. The 1 MΩ potentiometer is used as a vernier for selection of the exact cut-off current.

The current sensing circuit is used to turn the transmitter off whenever the current exceeds a specified value. This can happen when the unit is turned on at full power and a large mismatch, such as an improperly tuned tank circuit or a short across the output, is present.

There are two identical temperature sensing circuits, one for each of the zener diodes used in the power amplifier circuit. Each circuit consists of a simple differential amplifier. When the thermistor is cooler than 72°C its resistance is higher than 39K and the majority of the current flows through the opposite transistor. As the thermistor heats up, its resistance is lowered and at 72°C it becomes less than 39K and the current switches between the two transistors. This causes a voltage to be applied to the two SCR's and the transmitter is turned off.

The two power amplifier zeners that are monitored are extremely important in protecting the power amplifier transistors from the voltage spikes generated in the output transformer. They each absorb an average power of about 5 watts and have a normal operating temperature of 60°C with an ambient temperature of 20°C. If either zener fails the power transistors associated with that zener are destroyed in one cycle of operation, about 5μsec. There are conditions when an open circuit at the output will not result in excess current being drawn and thus the current sensing circuit will not shut the transmitter off. However, under this no-load or unbalanced load condition, the voltage spikes in the collector circuits become larger and have a longer duration. These higher energy spikes are absorbed by the zeners causing the zener temperature to rise rapidly. The sensing circuits shut the transmitter off when either zener reaches a temperature of 72°C. It may take up to 15 seconds of operation into an open or unbalanced load before the zeners heat up sufficiently, but no damage is done to the transmitter during this time interval.

The two SCR's are the devices that actually cause the transmitter to turn off. Both are fired simultaneously but each has a separate function. The disabling SCR, when fired, grounds point "W" of the modulator circuit and also completes the dc circuit for the multi-vibrator circuit causing the red fault lamps to flash sequentially. The grounding of point "W" disables the modulator circuit, turning the transmitter off. There is, however, considerable energy stored in the final drive circuit and up to several milliseconds are required for the output to drop to zero. The clamping SCR was added to decrease the turn-off time, which it does by grounding the keyed B+ lead thereby providing a path to ground for the stored energy.

Figure C-13 shows the waveform of the antenna terminals from the time the protective signal is applied to the gates of the SCR's. The time required for the SCR's to operate and for the output to drop to zero is less than 10 μsec.

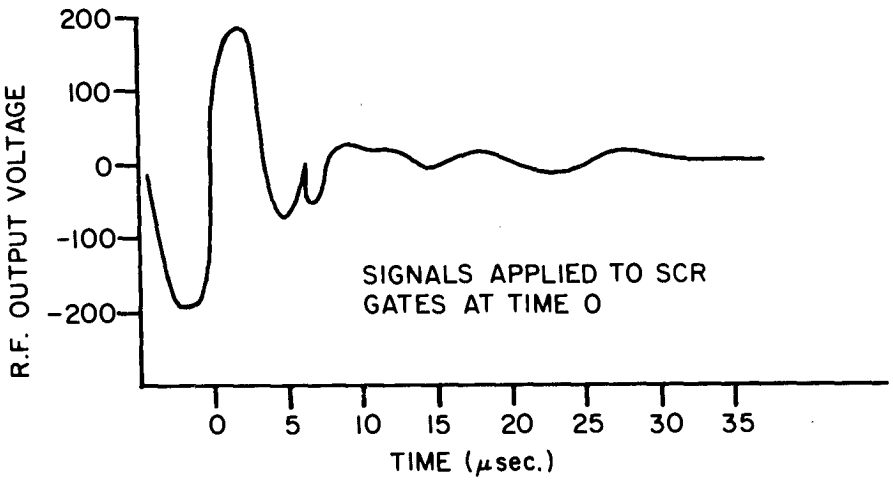

Fig. C-13. Transmitter output waveform after protective circuits are activated.

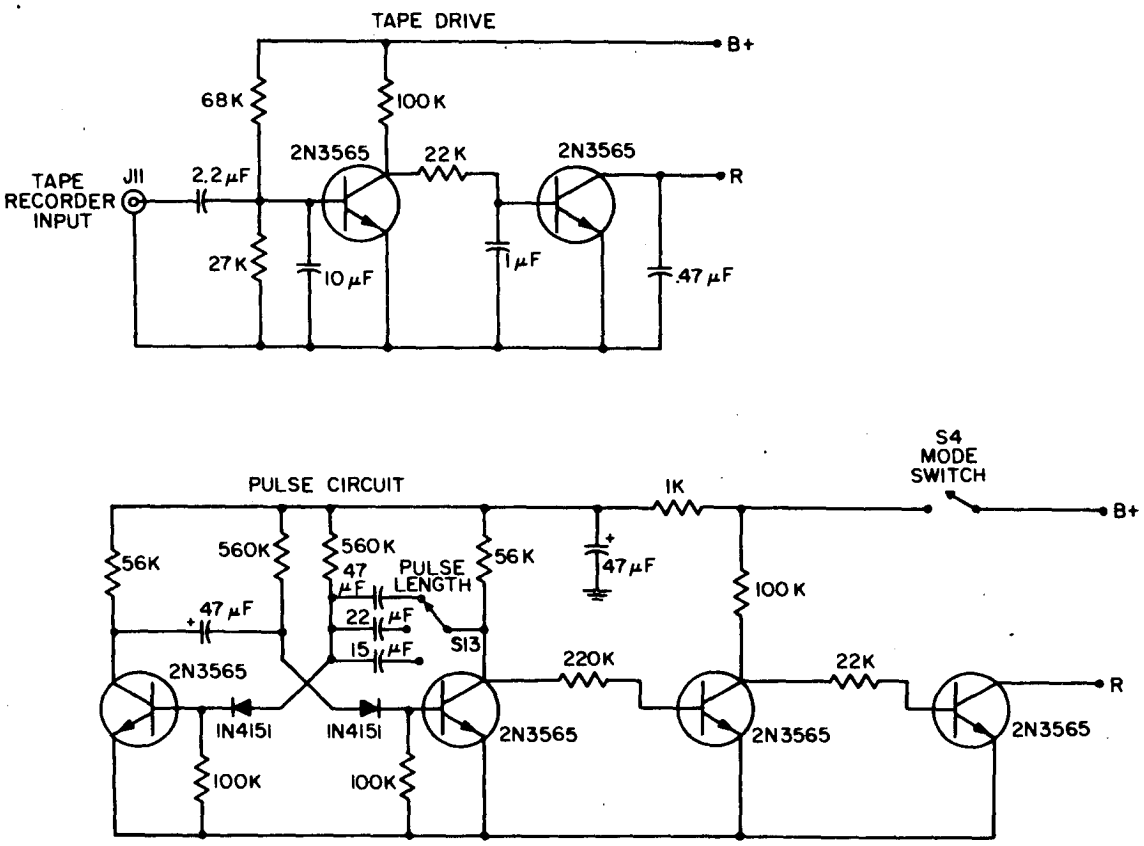

Fig. C-14. Transmitter auxiliary circuitry.

3.7 Auxiliary Circuits

During experimental work it is often necessary to have the transmitter operating automatically. A pulse circuit has been included to key the transmitter with selectable pulse lengths and a fixed repetition frequency. At other times it is desirable to send intelligence and, because of a scarcity of Morse code operators on our staff, a circuit has been included that will allow a tape recorder with recorded Morse code audio signals, to key the transmitter. Figure C-14 shows both circuits.

The 1 kHz Morse code pulses from the tape recorder are filtered by the 10 μF capacitor at the input so that the pulses switch the two 2N3565 transistors. The collector of the second transistor is connected to point "R" on the modulator circuit. Thus, when a dash or dot is played by the tape, the second transistor saturates and grounds point "R". This turns the transmitter on.

When the mode switch is out in the "pulse" position, B+ is applied to the pulsing circuit. The first section of the circuit is a multivibrator with one of the time constants variable. The other section is a saturating switch similar to the tape driver circuitry and the output is connected to point "R" of the modulation circuit. The time constants have been chosen to give a pulse interval of 20 seconds. The pulse lengths are variable by front panel control and can be either 5, 10 or 20 seconds long.

3.8 Transmitter System

Figure C-15 shows how all the above described circuits are connected together. The heavy line indicates the large current flow.

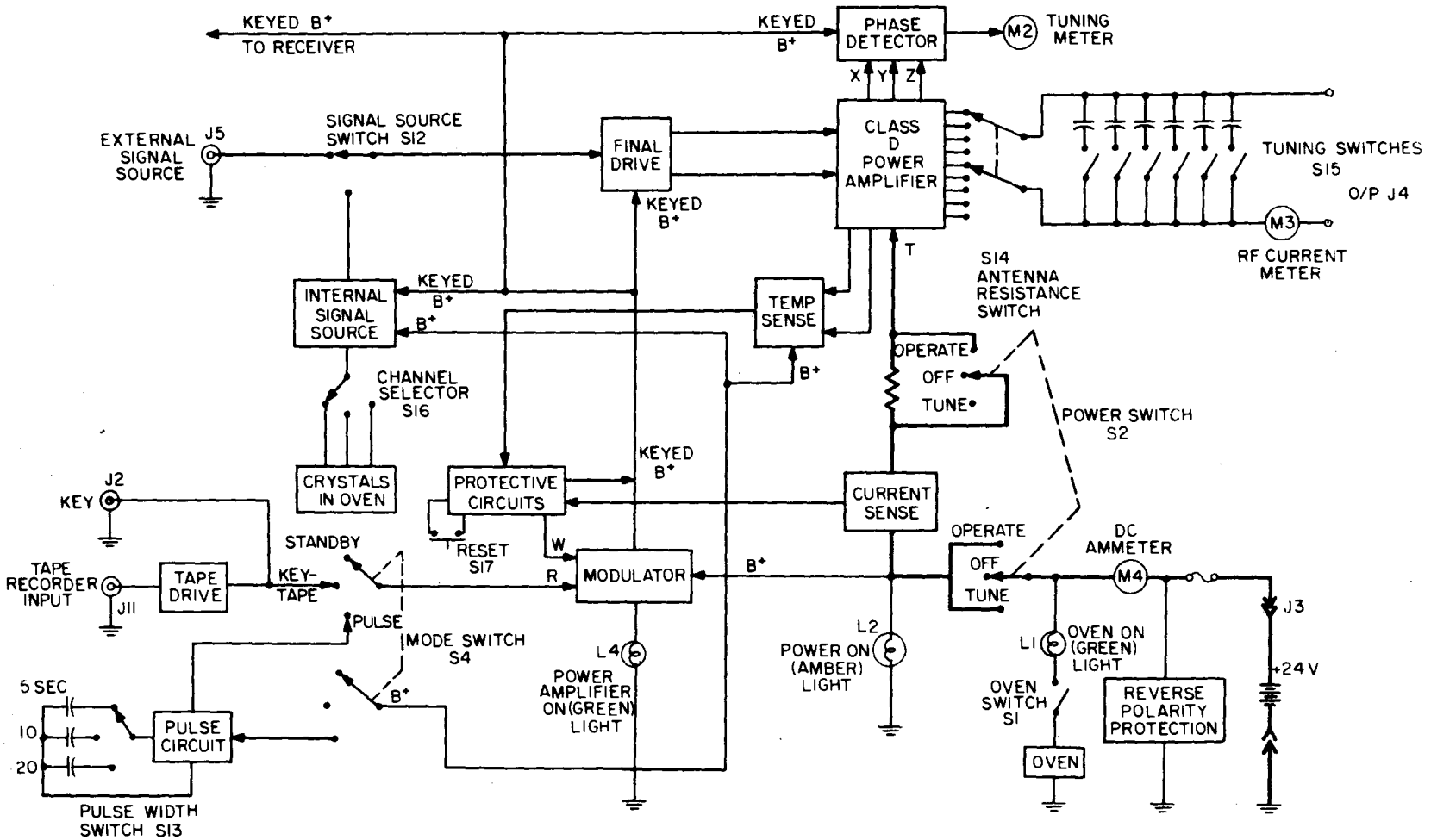

Fig. C-15. Transmitter system block diagram.

APPENDIX D

LOW FREQUENCY RECEIVER CIRCUIT DESCRIPTION AND PERFORMANCE CHARACTERISTICS

1. INTRODUCTION

Figure D-1 is a block diagram of the receiving system and, as can be seen, it is basically a double conversion super-heterodyne receiver. The system has three crystal controlled channels (110.75, 141.00 and 171.00 kHz) and three IF bandwidths (100, 500 and 2000 Hz) available, both parameters being selectable by front panel switches.

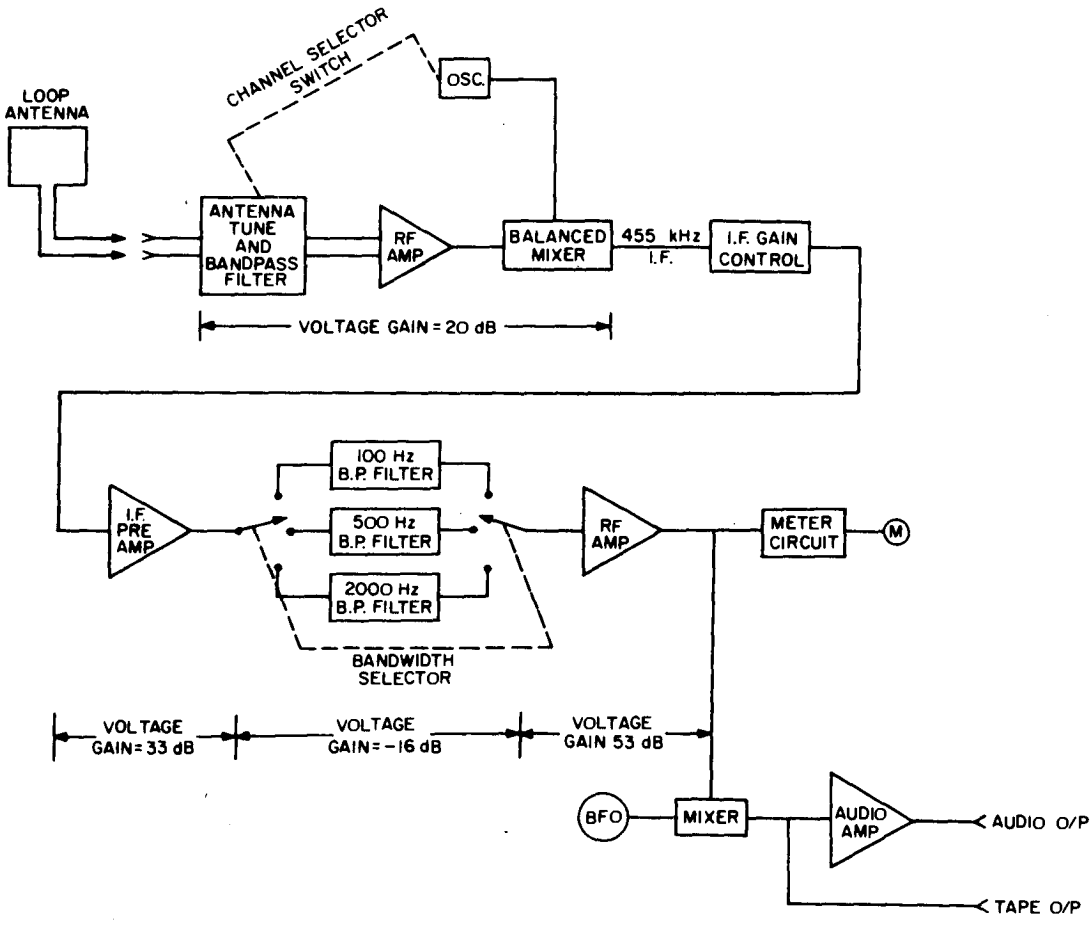

Fig. D-1. Receiver system block diagram.

The first IF frequency is 455 kHz while the second varies from 400 to 1200 kHz depending on the manual setting of the BFO control.

Considerable effort was employed in obtaining a low noise RF amplifier, a circuit not normally associated with low frequency receivers. However, in the arctic, particularly in the winter time, the external atmospheric noise level can be much lower than the thermal noise associated with the electrical circuits. Under these conditions, system sensitivity becomes limited by the internally generated noise and considerable gains in communications ranges can be obtained by lowering the noise figure of the receiver.

2. RECEIVER CIRCUITS

2.1 RF Stage

Figure D-2 is a schematic of the RF amplifier. The low noise transistors (2N2484) are connected in a balanced circuit and biased at an I_c of 1mA with V_{cc} set at about 5V. The output transformer in this circuit transforms the balanced 15K ohms output impedance to an unbalanced 50 ohm output. The two transformer windings are electrostatically shielded by a 0.002" brass sheet inserted between them. A ferroxcube 3B7 1-1/2" diameter potcore was used in winding the transformer. The amplifier has an overall voltage gain of 27 dB, and a noise figure of 3 dB. The input impedance is approximately 10K ohms.

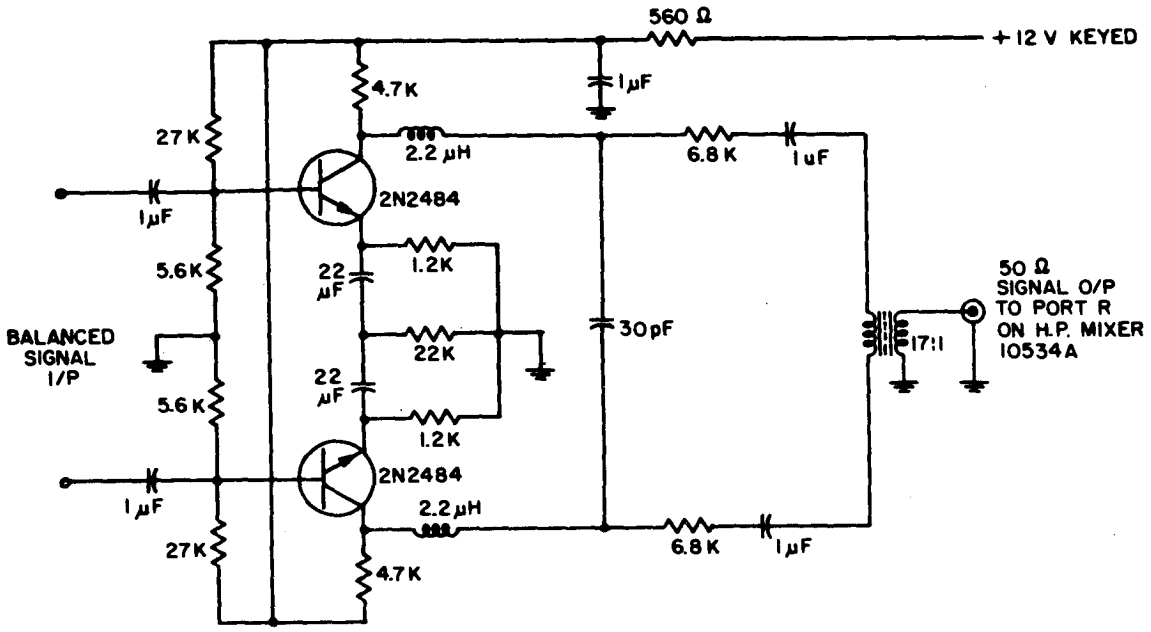

Fig. D-2. Receiver RF amplifier circuitry.

The +12V line to the RF amplifier is keyed by the transmitter modulation circuit. Thus when the transmitter is keyed on, the RF amplifier is turned off and when the key is off the receiver RF amplifier is turned on. This allows breakin operation requiring no mechanical switching when going from transmit to receive or vice-versa.

Figure D-3 shows the transfer characteristics for the RF amplifier and first mixer. The curve is linear from an input of -30 dB to +60 dB and substantially linear from -40 dB to +60 dB. The dynamic range is thus almost 100 dB, a characteristic extremely important for our application. For example, it is quite feasible for the receiver site to be located within 10 miles of some high powered LF beacons where the signal strength from the beacon can be as high as 10 millivolts/meter, or 80 dB>1 μV/m. If such an interference signal is within the fairly wide RF pass band (see Figure D-4) the non-linear portion of the transfer curve will cause mixing of the desired signal and the interference, and cross modulation will occur. If the signal is only 60 dB>1 μV/m no mixing and no cross-modulation will occur. It is thus seen that extension of the dynamic range is very important.

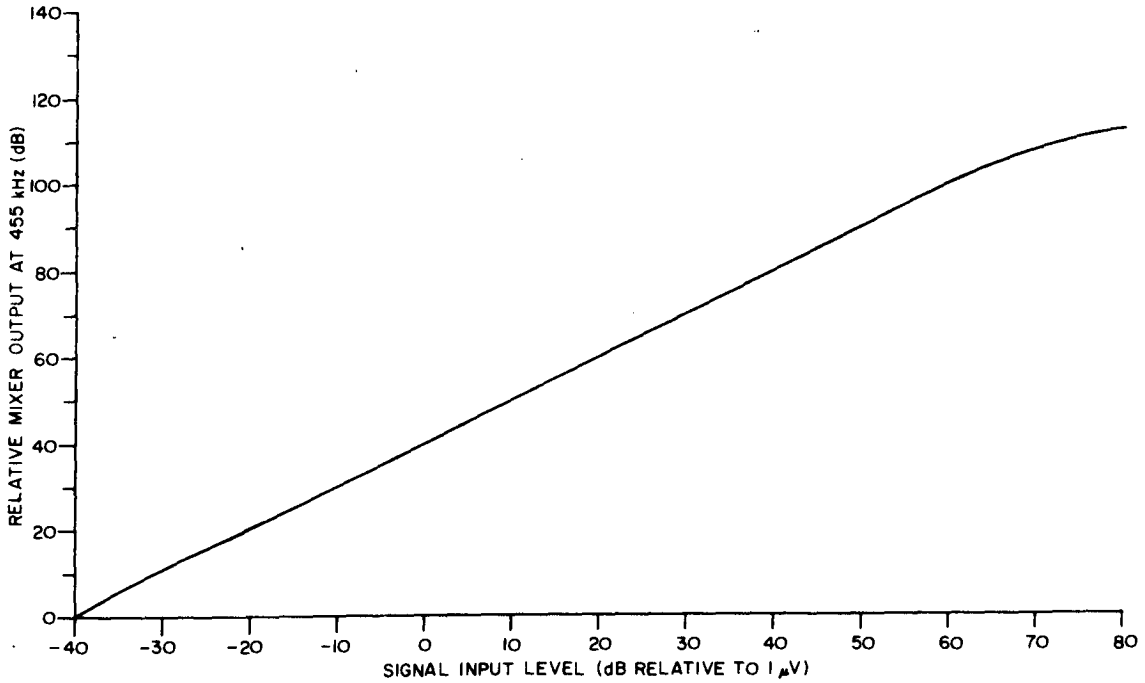

Fig. D-3. RF amplifier and first mixer transfer characteristic.

Figure D-4 is a graph of the RF bandwidth of the receiver. The characteristic is entirely due to the tuning of the loop antenna. The 3 dB bandwidth is 10 kHz, indicating that the loaded Q of the antenna circuit is about 14. A receiver design using a much narrower RF bandwidth would improve the interference rejection characteristics of the receiver.

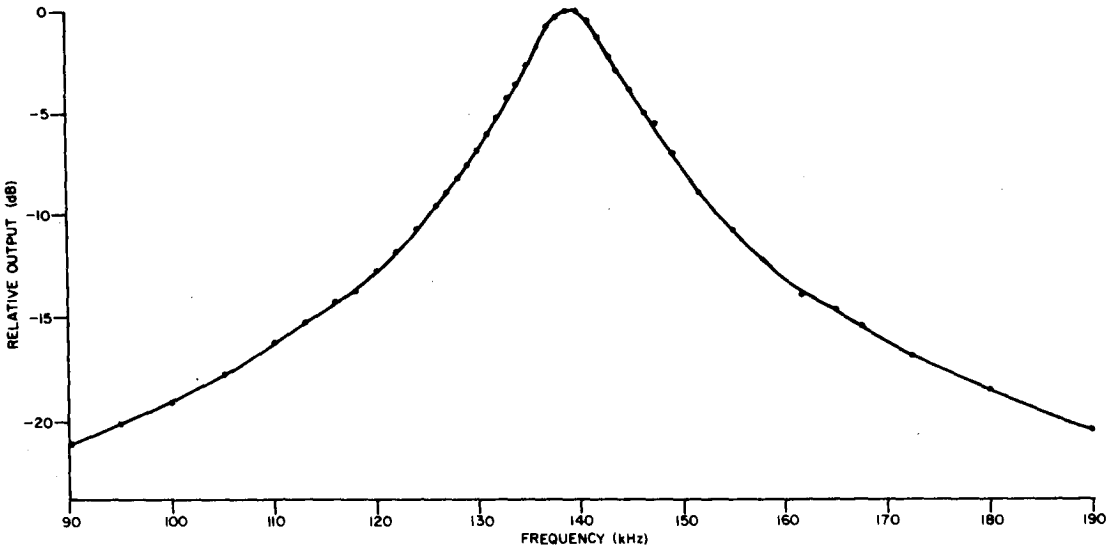

Fig. D-4. RF bandwidth of receiver at a center frequency of 141 kHz.

2.2 First Mixer Stage

The first mixer stage is passive and consists of a Hewlett-Packard balanced mixer, model No. 10534A. The R port is connected to the 50Ω output of the RF amplifier. The L-port is connected to the local oscillator which provides about one volt peak-to-peak to the mixer. The conversion loss of this mixer is 7 dB.

2.3 Local Oscillator

Figure D-5 is a schematic of the local oscillator. The circuit is very similar to the oscillator used in the transmitter except that there is no need for the frequency divider since crystals are available in HC-6/u holders in this frequency range. The oscillator frequencies are chosen to be 455 kHz above the signal frequency.

2.4 IF Stage 455 kHz

Figure D-6 is a schematic of the 455 kHz IF section of the receiver. The input from port X of the balanced mixer is applied to a 50Ω potentiometer which serves as the IF gain control. The first IF amplifier stage provides 33 dB gain. The insertion losses of the various filters have been equalized to 16 dB and the gain of the 2nd and 3rd IF amplifiers is 53 dB. Thus the overall gain of the IF section is 70 dB.

The first two IF stages are keyed ON and OFF in phase with the RF amplifier keying while the input to the third stage is shorted to ground by the diode switch whenever the transmitter is turned on. This switching arrangement effectively prevents any external signals from reaching the audio stages when the transmitter is keyed on.

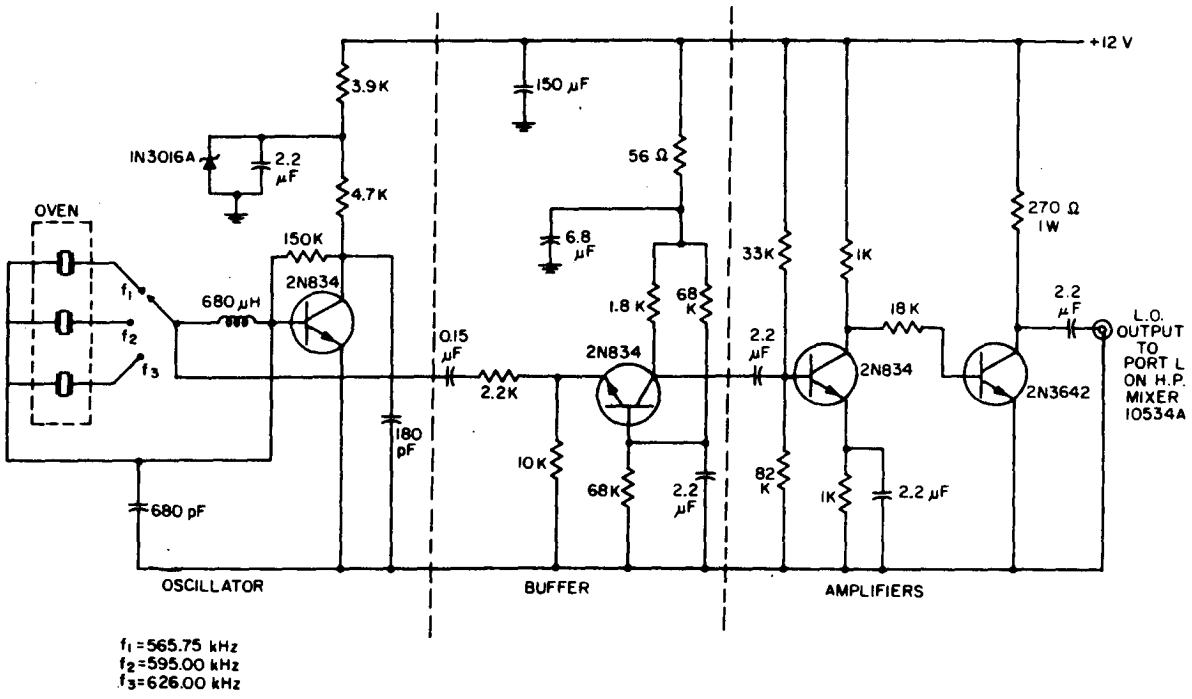

Fig. D-5. Receiver local oscillator circuitry.

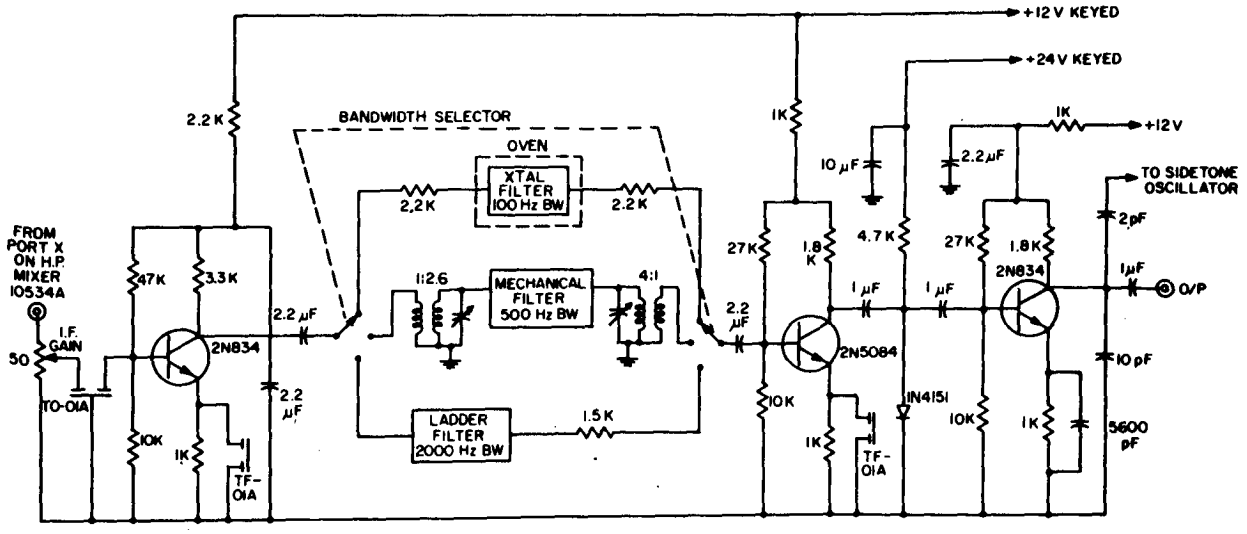

Fig. D-6. Receiver 455 kHz IF circuitry.

TO-01A and TF-01A are ceramic filters resonant at 455 kHz and are used here to improve the selectivity of the first IF stage.

Figure D-7 shows the transfer characteristics of the complete IF section. The curve was measured with the IF gain control set for maximum gain.

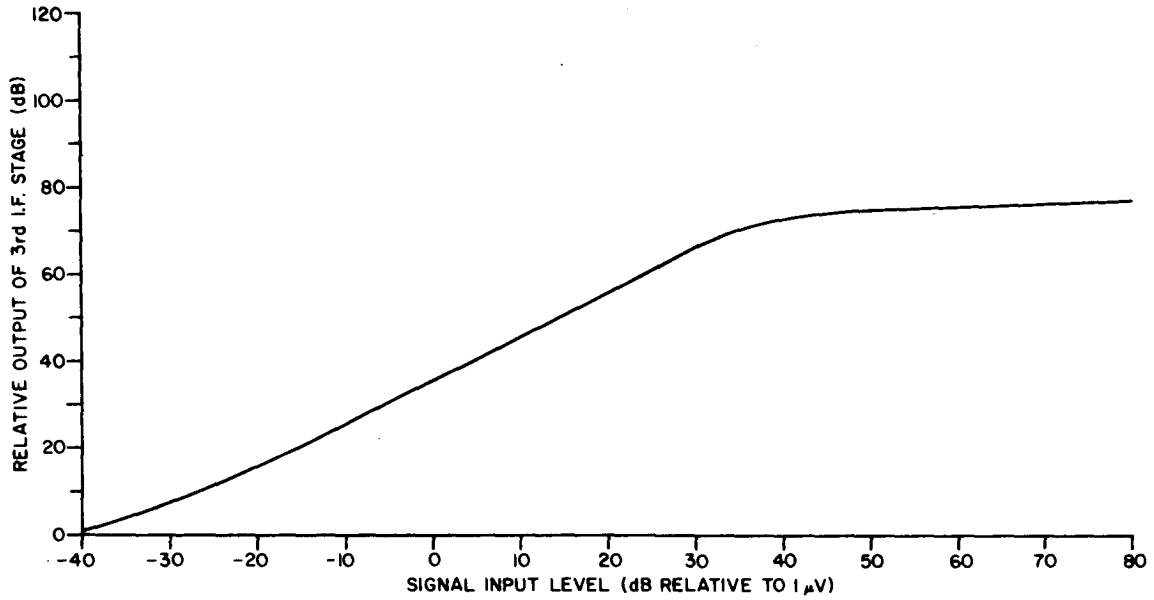

Fig. D-7. IF amplifier transfer characteristic.

2.5 2nd Mixer Stage

The mixer combines the 455 kHz IF signal and the BFO signal to produce an audio output. A dual gate FET transistor (3N141) is used as the active device and a conversion gain of 7 dB is realized. Figure D-8 is a schematic of this circuit. The 47 ohm resistor and 0.15 μF capacitor form a simple low pass filter which ensures that only audio frequencies are passed on to the audio amplifier.

2.6 BFO

Figure D-9 is a schematic of the BFO oscillator. The circuit uses a Clevite transfilter TO-01A as the major frequency determining element. With this type of circuit the BFO frequency can be adjusted over a wide range by means of a potentiometer. The oscillator has no shielding requirements and has a reasonably good temperature coefficient. The design of this type of circuit is outlined in reference (9). Figure D-10 shows the temperature characteristics of this oscillator.

2.7 Audio Amplifier

Figure D-11 is a schematic of the audio amplifier. The audio gain control adjusts the level of the signal applied to the final two stages. The output transformer changes the high output impedance to 600 ohms to match the earphone

impedance. The metering circuitry is connected to the output of the first stage. This makes the meter reading independent of the audio gain control.

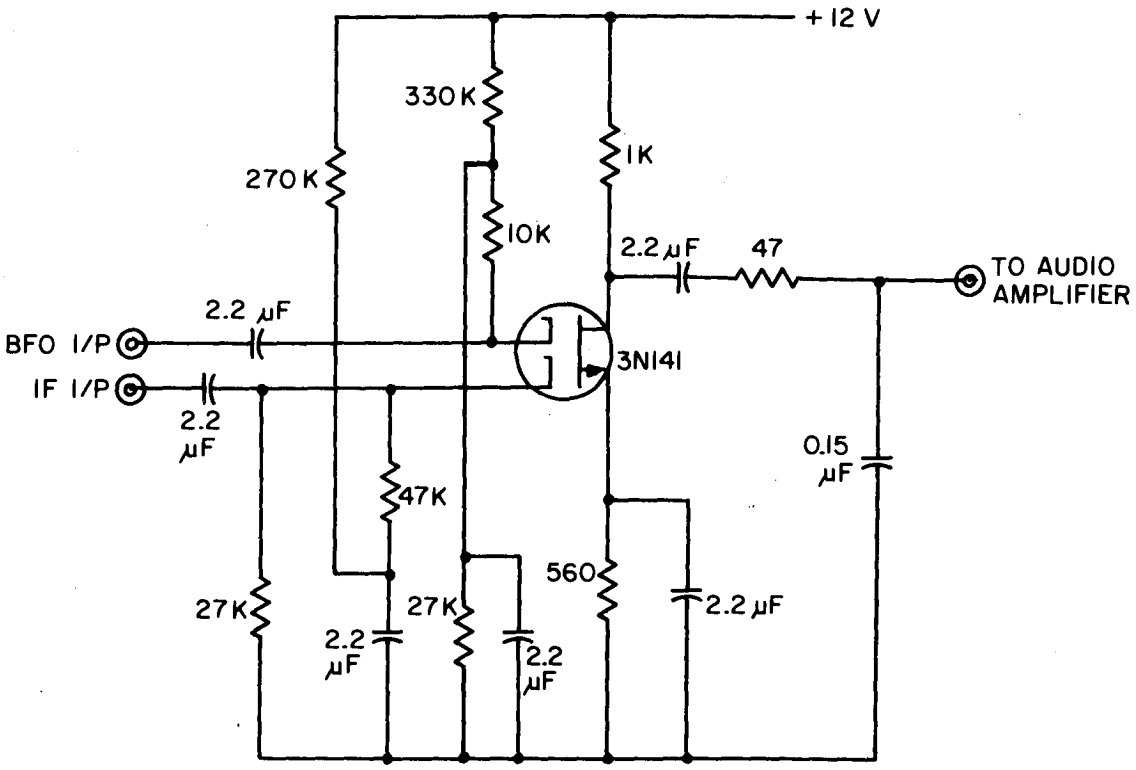

Fig. D-8. Receiver second mixer circuitry.

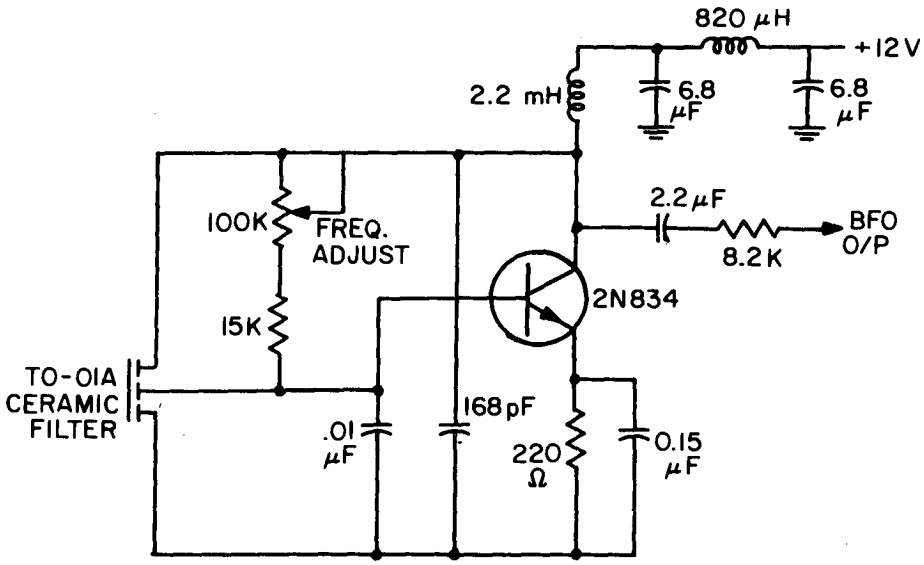

Fig. D-9. Receiver beat frequency oscillator circuitry.

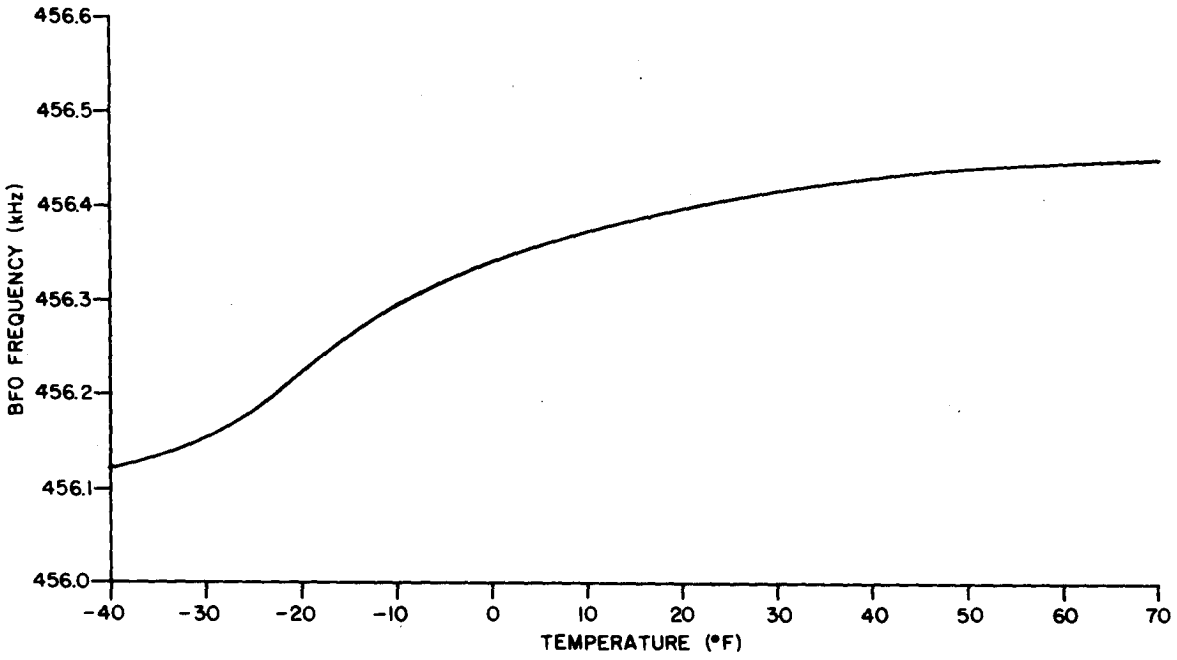

Fig. D-10. Receiver BFO frequency vs temperature characteristic.

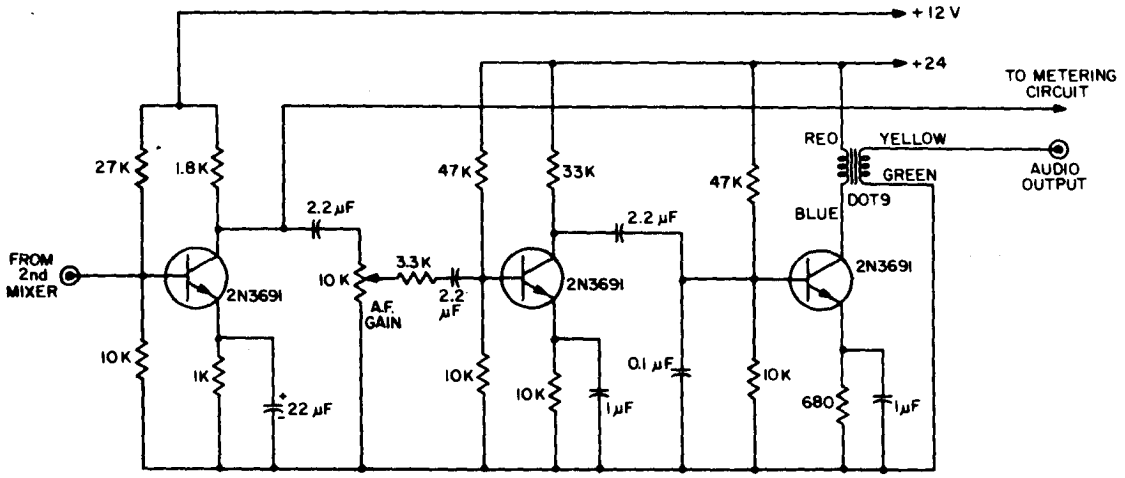

Fig. D-11. Receiver audio amplifier circuitry.

2.8 Metering Circuitry

The signal from the first audio amplifier is presented to the metering circuit shown in Figure D-12. The signal is filtered by the 47Ω resistor and 0.15 µF capacitor to make the meter response relatively flat over the frequency range of 200 to 1500 Hz. This reduces the effect of the BFO setting on the meter reading. The high input impedance FET amplifier is used to reduce loading on the audio circuits and is followed by a rectifier with a time constant of about 500 msec. The dc signal is amplified by the second FET and applied to the base of a differential amplifier pair. The meter is connected between the two emitters and has a reading proportional to the difference in base potentials.

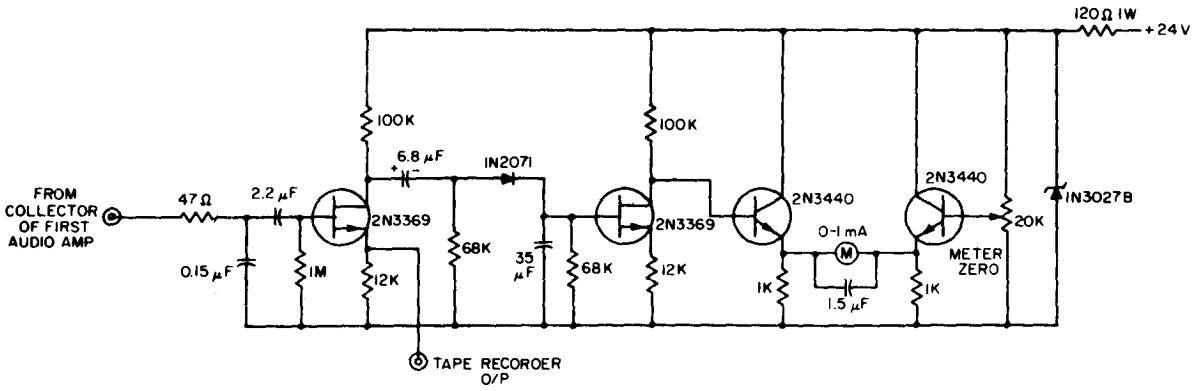

Fig. D-12. Receiver metering circuitry.

2.9 Sidetone Generator and Power Supply

Figure D-13(a) shows the sidetone generator that is used to give an audible tone in the earphones whenever the transmitter is keyed on. The output of this oscillator is capacitively coupled to the input of the second mixer. The frequency of the oscillator is crystal controlled to 456 kHz to give a one kHz audio tone. The oscillator is keyed 'ON' and 'OFF' in unison with the transmitter.

Figure D-13(b) shows the circuit which produces the various voltages used throughout the receiver. The primary source is a 24 volt battery and the keyed input from the transmitter is 0 volts when the transmitter is off and +24 volts when the transmitter is on. The 2N3440 inverts these voltages so that 0 volts from the transmitter causes +12 volts to be applied to the RF amplifier and first two IF amplifier stages, and +24 volts from the transmitter causes this voltage to be removed.

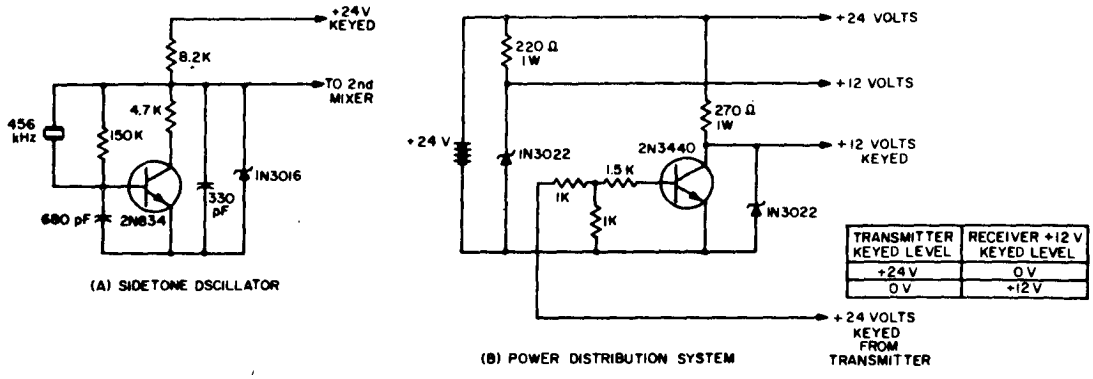

Fig. D-13. Receiver sidetone oscillator and power distribution circuitry.

3. RECEIVER PERFORMANCE MEASUREMENTS

3.1 Intermodulation

A two-signal RF test as described in reference (11) was conducted. It was found that two carriers at 170 kHz and 310 kHz each at a level of 74 dB> 1 μV produced an intermodulation product of 140 kHz equivalent in output level to a -16 dB> 1 μV input signal at 140 kHz. The receiver thus produces intermodulation products 90 dB below the carrier level. This result compares favorably with the 90 dB linear dynamic range of the RF amplifier.

3.2 Cross Modulation

A two-signal cross modulation test as described in reference (11) was conducted on the receiver with the 2000 Hz IF filter switched in. It was found that 10 per cent cross modulation is produced by a 30 per cent modulated interfering signal that is 60 dB above the desired signal voltage and 1.9 per cent removed in frequency from the desired signal.

3.3 Noise Modulation

The noise modulation test as described in reference (12) was conducted on the receiver with the 2000 Hz IF filter switched in. The results are plotted in Figure D-14. The top curve is the input/output characteristic with the signal generator modulated 30 per cent with a 400 Hz tone. The bottom curve is the same characteristic for an unmodulated carrier. It can be seen that increasing the unmodulated carrier causes an increase in the audio output. This is the result of noise modulation. The difference between the two curves at a given output signal level is the signal-to-noise ratio that would result when a signal of this level is applied to the receiver.

3.4 Effective Selectivity

Reference (12) describes a two-signal test to determine the effective selectivity of a receiver. This test provides information on the actual interference rejection characteristics of the receiver and the curves obtained are generally much wider than the IF rejection curve. Figure D-15 compares the IF rejection curve with the effective selectivity curve. Both curves are measured with the 2000 Hz IF filter in the circuit.

3.5 Temperature Effects

The entire receiver was tested over the temperature range from -40° to +70° F and the various critical receiver parameters were measured. Since the intended application for this unit calls for outdoor operation in the arctic, the low temperature characteristics are of considerable importance.

Figure D-16 shows the variation in receiver sensitivity as a function of temperature and with the 100 Hz IF filter connected. The sensitivity is degraded by one decibel by the low temperature.

Figure D-17 is a graph of the frequency stability of the receiver as a function of temperature. A ±5 Hz deviation from the center frequency is maintained over a temperature range of -37 to +50° F.

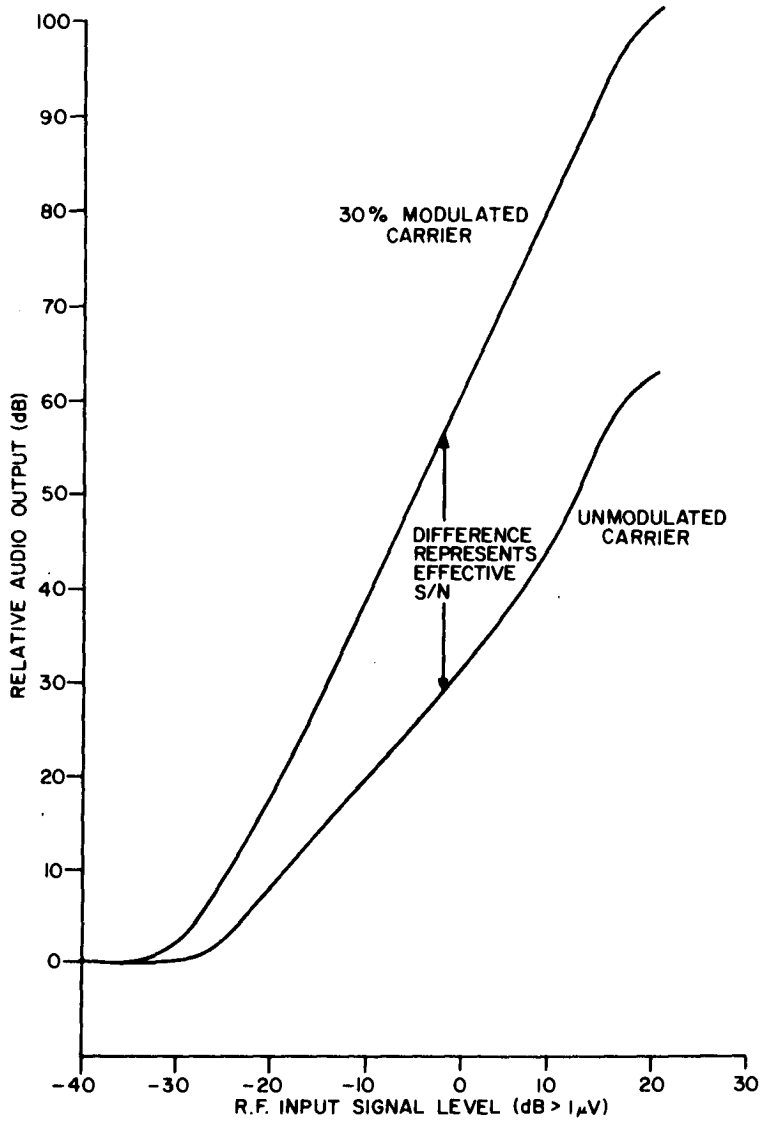

Fig. D-14. Receiver noise modulation characteristic for an IF bandwidth of 2 kHz.

Figure D-18 shows that the audio output level drops 5 dB as the receiver is cooled.

These tests indicate that the cold environment of the arctic should have very minor effects on the operation of the receiver system.

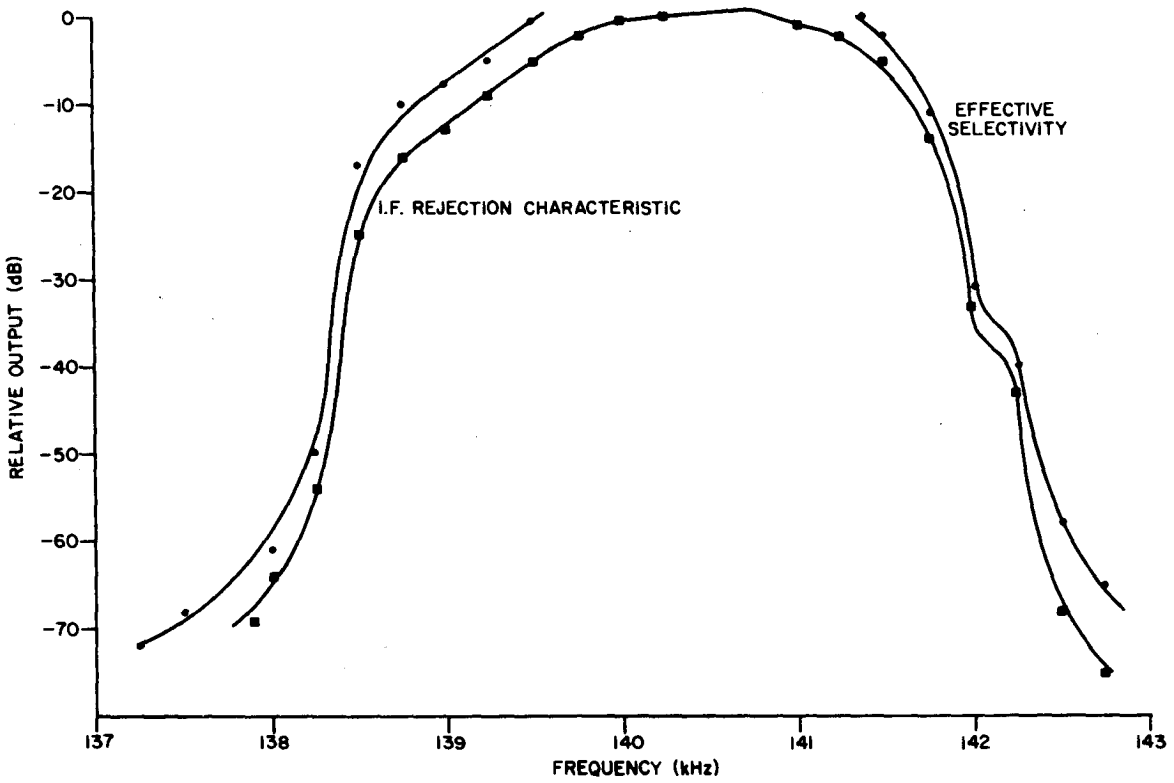

Fig. D-15. Comparison of IF filter rejection and effective IF bandwidth.

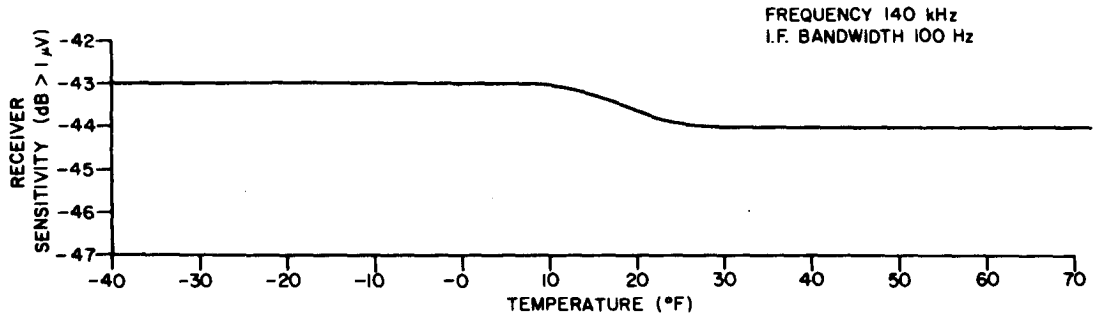

Fig. D-16. Receiver sensitivity as a function of temperature.

4. RECEIVING ANTENNA

4.1 Introduction

Man-made electrical noise is normally quite high in the inhabited parts of the arctic because adverse weather conditions affect the insulation associated with high tension line installations and the low ground conductivity prevents the establishment of efficient electrical grounds. For this reason, and because of high precipitation noise associated with blowing snow, it was decided to use a magnetic dipole antenna instead of an electric dipole. The

shielded loop antenna configuration provided the best means of implementing such a dipole. The theory of such loops and valuable practical advice in their construction is contained in reference (13). The design of the receiving loops used in this system is based on Belrose's work and on the information in reference (14).

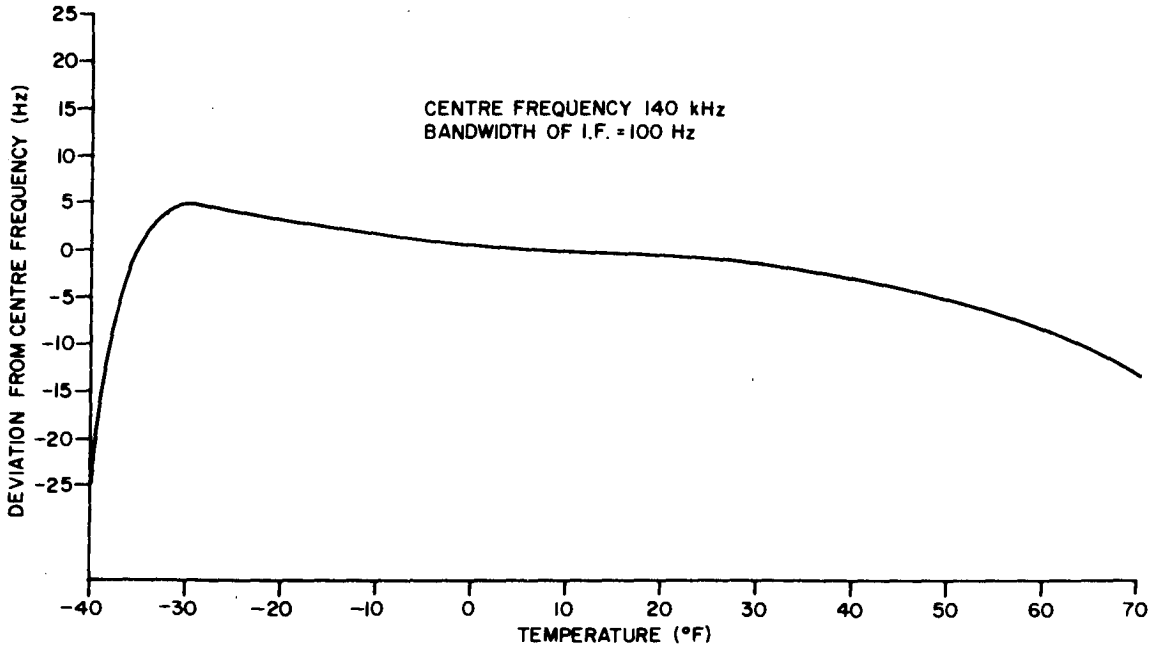

Fig. D-17. Receiver center frequency variations with temperature.

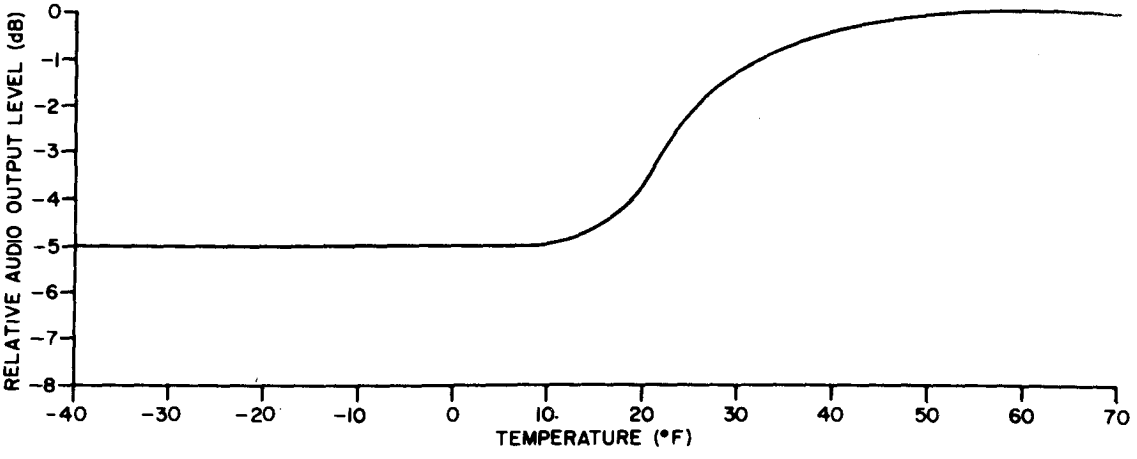

Fig. D-18. Receiver audio output variations with temperature.

A maximum physical size of 1 meter diameter was selected on the basis of portability and ease of use. From reference (14), the inductance of the loop, L_0 is given by:

$$L_0 = KA^{\frac{1}{2}} n^2 \times 10^{-6} \text{ Henries} \quad \ldots\ldots (1)$$

where
K is a constant depending on the form factor of the loop,
A is coil area in square meters,
and n is the number of turns in the loop.

If the coil width is 2 cm the diameter/width ratio is 50 and from the graph in reference (14), K = 3.5.

Therefore $L_0 = 3.1 \times n^2$ μH.

Using reference (13), it was decided to use a direct coupled loop antenna. It is desirable that the tuning capacitors required be of reasonable size and this determines the range of acceptable inductance for the loop. It was decided that a tuning capacitance of a few thousand picofarads would be acceptable and this meant that L_0 must be a few hundred microhenries. By choosing the number of turns, n, to be 12, L_0 becomes 446 μH. At 150 kHz, 2500 pF capacitance is required to resonate the loop.

The effective height of the loop antenna is calculated from the following formula from reference (14):

$$h_e = 2.094 \times 10^{-8} f A n \quad \ldots\ldots (2)$$

where h_e is in meters and f in Hz. Using the above parameters and a frequency 100 kHz,

$$h_e = 0.02 \text{ meters.}$$

Using reference (14), the power available from a direct coupled tuned loop is determined from the formula:

$$P_{out} = 8\pi^3 \times 10^{-14} f H^2 A^2 n^2 \frac{Q}{L_0} \quad \ldots\ldots (3)$$

where f is in Hz
H is the incident field intensity in ampere turns/meter,
and Q is the unloaded Q of the loop.

But since $L_0 \propto A^{\frac{1}{2}} n^2$, the available power out for matched and tuned conditions is independent of n but varies directly with $A^{3/2}$. A high Q loop is also helpful. For an incident signal of 1 μV/m at 100 kHz, the loop described above with an unloaded Q = 100 will have an available power out of -136 dBm.

The receiver described in this appendix has a 3 dB noise figure, giving a sensitivity of -151 dBm for a 100 Hz bandwidth and thus the overall system sensitivity is 151-136 = 15 dB<1 μV/m.

4.2 Construction

The loop antenna constructed for this system has a mean diameter of 39 inches and is constructed from $1\frac{1}{4}$ inch aluminum tubing. There is a 2 inch insulated section at the top and all connections are made at the base of the antenna. Twelve turns of litz wire are mounted on a phenolic board inserted into the tubing. The ends of the loop are connected to a twin coaxial connector and the centre point is grounded to the shield.

Figure D-19 shows the schematic of the loop and the measured parameters. Included in the schematic is the calibration transformer used to calibrate the system.

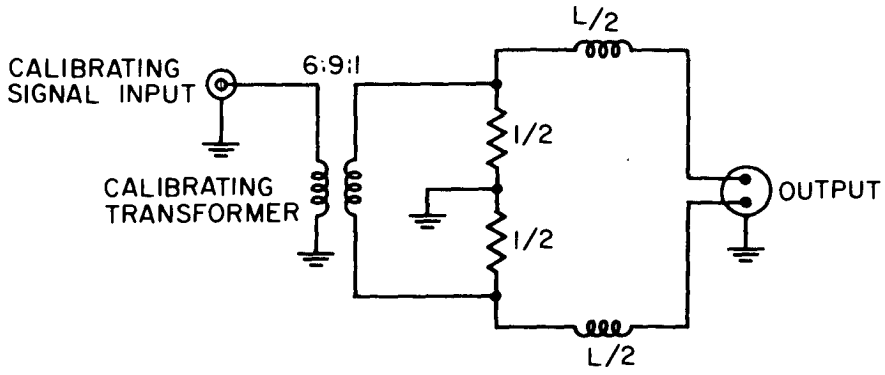

MEASURED PARAMETERS

LOOP INDUCTANCE (L) _____ 420 μH
UNLOADED Q _____ 85
EFFECTIVE HEIGHT AT 100 kHz _____ 0.02 METERS

Fig. D-19. Receiver loop antenna schematic.

EVANS, W. M.
--A transportable low frequency
communications system.